Acta Geologica Polonica, Vol. 74 (2024), No. 3, e18
DOI: 10.24425/agp.2024.150010

Morphometrics of the mandible of *Metoposaurus krasiejowensis* Sulej, 2002 and its ecological implications

LUCA F. QUARTO[1] and MATEUSZ ANTCZAK[2]

[1] *University of Opole, European Centre of Palaeontology, Oleska 48, 45-052 Opole, Poland; e-mail: lucaquarto1998@gmail.com*
[2] *University of Opole, Institute of Biology, Oleska 22, 45-052 Opole, Poland; e-mail: mateusz.antczak@uni.opole.pl*

ABSTRACT:

Quarto, L.F. and Antczak, M. 2024. Morphometrics of the mandible of *Metoposaurus krasiejowensis* Sulej, 2002 and its ecological implications. *Acta Geologica Polonica*, **74** (3), e18.

Amphibians, due to their ecological plasticity, are some of the best environmental indicators among vertebrates nowadays and in the fossil record. One such example is the extinct family Metoposauridae Watson, 1919. Metoposaurids were abundant amphibians in Late Triassic Pangea. The remains of the genus *Metoposaurus* Lydekker, 1890 have been found in Germany, Poland and Portugal with three species, respectively *Metoposaurus diagnosticus* (Meyer, 1842), *Metoposaurus krasiejowensis* Sulej, 2002 and *Metoposaurus algarvensis* Brusatte, Butler, Mateus and Steyer, 2015. Since the majority of studies concern the skull and the pectoral girdle, in this work *M. krasiejowensis* has been analysed through a morphometric study of the mandible. This was made possible by the high abundance of fossils found in Krasiejów (SW Poland) in the last 20 years. The characteristics considered are the morphology of the mandible corpus and its most relevant bones, the adaptation to stress during biting and the dermal ornamentation. The results reveal that not only do these characters have great intraspecific variability, but that at least two groups of a single population of *M. krasiejowensis* probably had different lifestyles, one more aquatic and the other more terrestrial.

Key words: Temnospondyli; Metoposaurids; Mandible; Morphometrics; Dermal bone ornamentation; Palaeoecology.

INTRODUCTION

In the Late Triassic, metoposaurids (Yates and Warren 2000) were common and diversified amphibians, among the most abundant non-marine vertebrates. In Europe the genus *Metoposaurus* Lydekker, 1890 has been found in Germany (Meyer 1842; Fraas 1889; Lydekker 1890; Milner and Schoch 2004), Poland (Sulej 2002, 2007), and Portugal (Witzmann and Gassner 2008; Brusatte *et al.* 2015). The German material was the first to be described as *Metopias diagnosticus* Meyer, 1842 (Meyer 1842; Fraas 1889) and later as *Metoposaurus diagnosticus* (Lydekker 1890). After the finding of new specimens in Poland and Portugal, the presence of some different characters, mainly concerning the skull or the pectoral girdle, i.e., the location of the lacrimal and ornamentation of clavicles and interclavicles (Sulej 2007), led to the identification of two different species: *Metoposaurus krasiejowensis* Sulej, 2002 and *Metoposaurus algarvensis* Brusatte, Butler, Mateus and Steyer, 2015.

The abundance and the diversity of bones in Krasiejów (SW Poland) have, in the last 20 years, made *M. krasiejowensis* an interesting case for biochronological, osteological and histological studies (Sulej 2002, 2007; Barycka 2007; Konietzko-Meier and Wawro 2007; Lucas *et al.* 2007; Konietzko-Meier and Sander 2013; Antczak and Bodzioch 2018; Konietzko-

Meier *et al.* 2018; Teschner *et al.* 2018; Gruntmejer *et al.* 2019a, b, 2021; Lucas 2020; Kalita *et al.* 2022).

Several studies have indicated the possibility of distinguishing two groups inside the population of *M. krasiejowensis*, with osteological differences due to ecology or sexual dimorphism. The majority of these studies concerned the skull, the pectoral girdle and long bones. In this work, instead, we verify if this variation can be found also in the lower jaw through two approaches. With the aim of seeing if the morphometrical differences are real and consistent among the specimens, numerous dimensions have been measured, and accurate descriptions made of the symphysial region, the openings, the pits and the dermal bone ornamentation. On the other hand, we have tested their possible impact on the adaptation to stress during biting, with the mandibular force profile method. The data were also compared with ones of another temnospondyl found in Krasiejów, *Cyclotosaurus intermedius* Sulej and Majer, 2005, whom mandible is almost identical to that of *M. krasiejowensis*, except for its having a more prominent hamate process and a major general size. We provide an explanation about these morphological differences based, above all, on the analysis of the dermal bone ornamentation.

THE MANDIBLE OF METOPOSAURUS

Anatomy of the mandible

The lower jaw of *M. krasiejowensis* (Text-fig. 1) has a narrow, tubular structure with the dentary in anterodorsal and labial position, three coronoids and the prearticular on the lingual side, splenial and postsplenial on the ventrolingual side and angular and surangular in the posterolingual position. The lingual side presents a large Meckelian window and other accessorial openings (henceforth the intermeckelian foramen, the anterior Meckelian window, and other accessory foramina and pits are indicated as accessory openings) while the adductor fossa is on the dorsal side, between the coronoid and the hamate processes. The teeth lie only on the dentary, except for the tusk on the symphysial plate and the parasymphysial teeth on its lingual margin (Sulej 2002, 2007). This structure is common among all the stem tetrapods and tetrapodomorph fishes (Ahlberg and Clack 1998; Anderson *et al.* 2013), with some exceptions, e.g., species with teeth on coronoids, species with less numerous coronoids and species with a small Meckelian window (Clack *et al.* 2012). These small variations are diagnostic for recognition of the species, and sometimes mandibles are the only remains of primitive tetrapods (Ruta and Bolt 2008). Nevertheless, the overall shape of all these mandibles with numerous bones, elongated shape, low and backward processes and a large symphysial tusk can be simplified in order to analyse the mechanical behaviour of tetrapods mandible.

A simple, hypothetical model made by Olson (1961) considers only the mandible bones and two muscular groups, the adductor mandibuli muscle and the pterygoideus muscle, and distinguishes two systems. The early tetrapods, as far as the temnospondyls, which are generally characterised by a large, flat skull close to the girdle, belong to the kinetic inertial system. Here the muscular groups form a right angle with the mandibular corpus when the mouth is open and at this time the muscles exert their maximum force to instantly close the mouth and impale the prey with tusks, through a snapping movement. In basal amniotes instead, which have a smaller and narrower skull than primitive tetrapods, the tusk is reduced or lost, coronoid teeth disappear, the coronoids themselves are reduced or lost and the muscle groups form a right angle when the mouth is almost closed, to exert the highest force to hold the prey tightly, with a squeezing action. This model is called a static pressure system. In this study, a model that works as in the kinetic inertial system is used to perform the mandible force profile method, based on beam theory.

Beam theory and biomechanical model of the mandible

According to beam theory, if a cantilevered beam undergoes a bending load, the bending results in tensile stress on the side on which the load is applied and compressive stress on the opposite side (Biewener 1992; Text-fig. 2B). Along the neutral axis that passes through the centroids of the sections of the mandible there is no stress. The mandible can be modelled as a cantilevered beam that undergoes bending loads during biting, depending on the position and force of the muscular group. The bite force applied at any point on the mandible reflects its external dimensions in each location. Then, the variation of these dimensions indicates the ability of the mandible to resist different loads, which reflects the feeding behaviour (Therrien 2005a, b; Therrien *et al.* 2005, 2016).

This model is based on the assumption that the mandible section is perfectly elliptical and solid. Each section has its shape and can present hollows on the surface, such as the Meckelian window or the abduc-

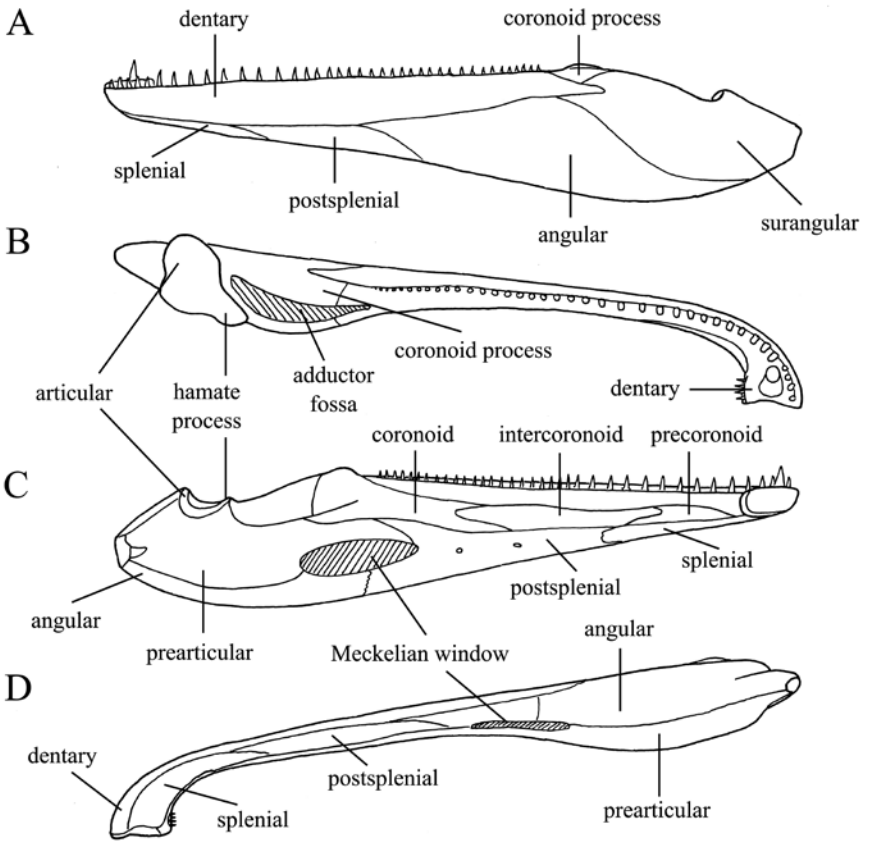

Text-fig. 1. Schematic representation of the bones of the mandible of *Metoposaurus krasiejowensis* Sulej, 2002, without the ornamentation, on A – labial side; B – dorsal side; C – lingual side; and D – ventral side. The mandible has a narrow, tubular structure with the dentary in antero-dorsal and labial position, three coronoids, without teeth, and the prearticular on the lingual side, splenial and postsplenial on the ventrolingual side, angular and surangular in the posterolingual position. The lingual side presents a large Meckelian window and other accessorial openings, while the adductor fossa is on the dorsal side, between the coronoid and the hamate processes.

tor fossa, and, above all, inside. Therefore, besides beam theory (Biknevicius and Ruff 1992; Therrien 2005a, b; Therrien *et al.* 2005, 2016; Organ *et al.* 2006), other biomechanical approaches have been developed, such as jaw musculature reconstruction (Christiansen and Adolfssen 2005; Christiansen and Wroe 2007; Wroe *et al.* 2007) and finite element analysis (FEA) (McHenry *et al.* 2007; Rayfield 2007; Fry *et al.* 2009; Slater *et al.* 2009, 2010; Tseng and Binder 2010; Tseng and Wang 2010; Tseng *et al.* 2011; Fortuny *et al.* 2012; Tseng 2013; Figueirido *et al.* 2014; Konietzko-Meier *et al.* 2018; Rowe and Snively 2022). However, the mandibular force profile method, based on beam theory, remains the simplest, because it does not require computer tomography (CT) or scanners; its results are quite similar to the ones of FEA and it can be used to substitute or integrate other techniques as well (Metzger *et al.* 2005; Walmsley *et al.* 2013; Therrien *et al.* 2016; Rowe and Snively 2022). The mandibular force profile method is mainly used with crocodilians (Busbey 1995; Metzger *et al.* 2005; McHenry *et al.* 2006; Walmsley *et al.* 2013) and theropods (Therrien *et al.* 2005; Snively *et al.* 2006; Cuff and Rayfield 2013) to examine the adaptation of the skull and mandible to stress in biting, shaking and twisting. In this work we do not investigate the possibility of *Metoposaurus* performing lateral or rotational movements; we just apply the method to biting to verify if it can be useful to understand the differences among specimens or add information about the general functioning of the mandible.

Dermal bone ornamentation

Many vertebrates, including arandaspids (Young 2009), heterostracans and osteostracans (Märss 2006), placoderms (Giles *et al.* 2013), actinopterygians (Lundberg and Aguilera 2003), and basal tet-

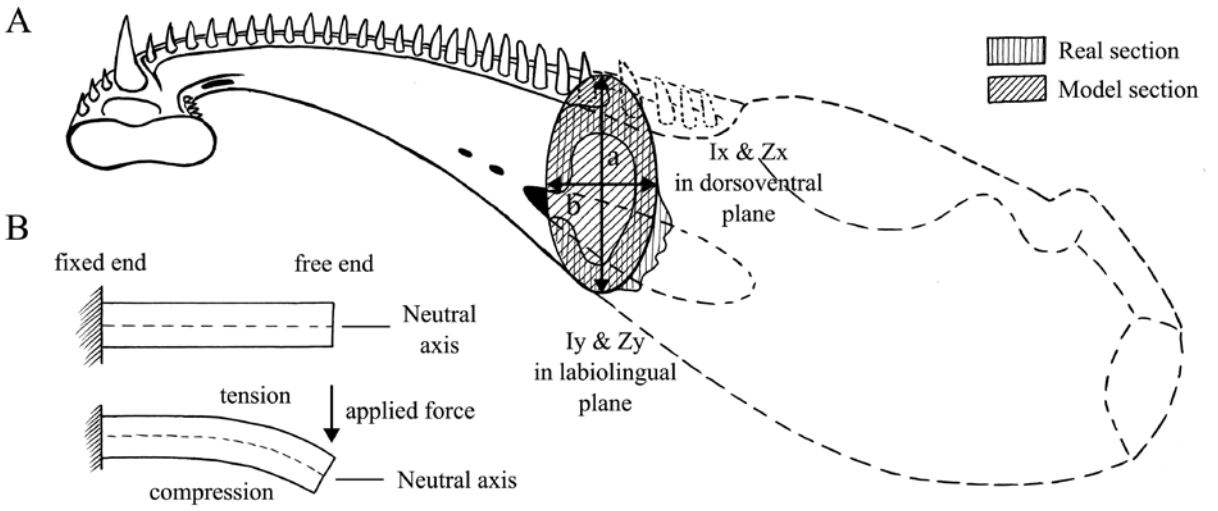

Text-fig. 2. A – Simplified representation in perspective of the *Metoposaurus krasiejowensis* Sulej, 2002 mandible with the elliptical section and the axes. The section is perpendicular to the longitudinal axis of the corpus and approximates the form of the real section, without considering holes and possible irregularities in the dermal bone ornamentation on the labial side. B – Behaviour of a beam without and with a load applied to the free end.

rapods, such as *Eusthenopteron* Whiteaves, 1881 (Zylberberg *et al*. 2010), *Panderichthys* Gross, 1941 (Vorobyeva and Schultze 1991), *Elpistostege* Westoll, 1938 (Schultze and Arsenault 1985), *Tiktaalik* Daeschler, Schubin and Jenkins, 2006, temnospondyls (Meyer 1858; Credner 1881; Fraas 1889; Fritsch 1889; Zittel 1911; Bystrow 1935, 1947; Romer 1947; Cosgriff and Zawiskie 1979; Boy and Sues 2000; Schoch 2001; Dias and Richter 2002; Witzmann *et al.* 2010; Witzmann and Soler-Gijón 2010; Rinehart and Lucas 2013a; Antczak and Bodzioch 2018), but also crocodilians (De Buffrénil 1982; Clarac *et al.* 2015; De Buffrénil *et al.* 2015; Pochat-Cottilloux *et al.* 2023), squamates (De Buffrénil *et al.* 2011) and turtles (Scheyer *et al.* 2007), present a dermal bone ornamentation. The ornamentation, or sculpture, is composed of pits, ridges, tubercles and furrows, and covers the outer surface of the bones in the skull roof, lateral side of the mandible, pectoral girdle and osteoderms, forming repetitive, non-random geometrical patterns. Despite the fact that this character is widespread and has been recognised since the 19th century (Credner 1881), its functional significance remains poorly understood.

Bystrow (1935) distinguished between a polygonal ornamentation that first forms ontogenetically in the ossification centre and a radial ornamentation that follows the direction of growth of the bone. He also interpreted the pores within the pits as a capillary network used for cutaneous respiration by aquatic stem tetrapods (Bystrow 1947). Following the approach of Credner (1881) and Bystrow (1935), the ornamentation has been used to distinguish the different ontogenetic phases in temnospondyls (Boy and Sues 2000), but several other hypotheses have been proposed: increasing the mechanical resistance of the skull by distributing the stress during feeding (Coldiron 1974; Rinehart and Lucas 2013a); reduction of water loss by evaporation (Seibert *et al.* 1974); augmenting the skin anchorage and strengthening and surface area (Romer 1947; Cosgriff and Zawiskie 1979; Schoch 2001; Dias and Richter 2002; Witzmann and Soler-Gijón 2010); increasing basking efficiency (Seidel 1979); and contributing to acidosis buffering and lactic acid build-up due to anaerobic activity (Janis *et al.* 2012).

In tetrapods and, in particular, in temnospondyls, two types of ornamentation are prevalent (Witzmann *et al.* 2010; Rinehart and Lucas 2013a). The former, called polygonal or reticulate, is composed of cells with four, five or six sides or rounded shapes. Each cell has a concave, approximately flat-bottomed area, the pit, enclosed by ridges. The bottom of each cell contains at least one vascular opening. The points of intersection of the ridges are called nodal points and if they are higher and broader than the ridges, they are designated as tubercles. Sometimes this is called 'honeycomb-' or 'waffle-iron-like' texture. The latter, the radial, presents parallel or sub-parallel, longitudinal and round-bottomed grooves, separated by

ridges. The vascular openings are often accompanied by an axilla ridge. The surface of both types of ornamentation can also present some small pores. In this study the vascular openings and the pores are not taken into account.

GEOLOGICAL SETTING

The Upper Triassic (Keuper) of the German Basin is a thick, regressive, fine-siliciclastic succession in Central Europe, extending from western France to eastern Poland. In Poland, the Upper Silesian Keuper facies outcrops in a few localities. One of them is an abandoned open-cast mine of claystones and siltstones near Krasiejów in the Opole voivodeship. While in Germany the Keuper is divided into three parts, i.e., lower, middle and upper, in Poland it is divided into two parts: the lower part of the succession has been correlated with the late Carnian 'Upper Gypsum Series' and the upper part with the 'Lisów Breccia' (Bilan 1975), but also with the middle or upper Norian Jarkowo Beds or Zbąszynek Beds (Grodzika-Szymanko 1971; Mader 1997). The chronostratigraphic position of the upper part remains uncertain and its fossil content cannot provide more information, thus Carnian (Dzik and Sulej 2007; Lucas 2015) and Norian (Środoń *et al.* 2014; Fijałkowska-Mader 2015; Racki and Szulc 2015; Szulc *et al.* 2015a, b) attributions are both plausible. The bonebeds were correlated with the German Carnian Untere Bunte Mergel Formation (Dzik 2001, 2003), and the Norian Drawno Beds (Sulej 2002). More recently, three lithostratigraphic members have been formally defined: the Ozimek (Mudstone-Evaporite) Member, the Patoka (Marly Mudstone-Sandstone) Member and the Woźniki (Limestone) Member. The bone-bearing horizon of Krasiejów belongs to the Patoka Member (Szulc *et al.* 2015a). The succession that contains the vertebrate bonebeds can be divided into three sedimentary units: two alluvial units with siltstone and channels that represent low-energy environments, respectively an anastomosing river for the lower unit and a meandering river for the upper unit, and a lacustrine unit between these two alluvial units, with massive claystone that represents an extensive lake existing in a warm, subtropical climate with an arid-to-wet seasonal rhythm (Gruszka and Zieliński 2008). Among the three units lie two bone-bearing horizons: the lower with *M. krasiejowensis* and the upper with *Silesaurus* Dzik, 2003 and *Polonosuchus* Brusatte, Butler, Sulej and Niedźwiecki, 2009 (Dzik and Sulej 2007).

MATERIALS AND METHODS

All the specimens are deposited in the Institute of Biology at the University of Opole. For morphometric measurements, 33 numerical variables (Table 1) and 7 categorical variables (Table 2) have been measured on 22 specimens of *M. krasiejowensis* and

antp	Length of the anterior accessory opening
l1	Total length along the major axis
l2	Total length along the labial margin
ld	Length of the dentary
h1	Depth at the articular
h2	Depth at the hamate process
h3	Maximum depth (coronoid process or near)
w1	Maximum width (coronoid process or near)
w2	Minimum width (generally near the point of maximum curvature)
h5	Depth in suture between dentary and surangular
w4	Width in suture between dentary and surangular
h6	Depth in half dentary (for specimen without symphysial region the length of the dentary has been calculated based on specimens with similar length)
w5	Width in half dentary (for specimen without symphysial region the length of the dentary has been calculated based on specimens with similar length)
h4	Depth in the symphysis
w3	Width in the symphysis
h10	Depth at the second tooth alveolus
w6	Width at the second tooth alveolus
l6	Distance between the second tooth alveolus and the middle of the articulation
l7	Distance between the middle of the dentary and the middle of the articulation
l8	Distance between the dentary-surangular suture and the middle of the articulation
l9	Distance between the section of maximum depth and the middle of the articulation
hm	Height of Meckelian window
m	Width of Meckelian window
d1	Distance between the Meckelian window and the first accessory opening
h7	Height of the first accessory opening
l3	Width of the first accessory opening
d2	Distance between the first and the second accessory opening
h8	Height of the second accessory opening
l4	Width of the second accessory opening
d3	Distance between the second and the third accessory opening
h9	Height of the third accessory opening
l5	Width of the third accessory opening
a	Length of the abductor fossa
wa	Width of the abductor fossa

Table 1. Numerical variables of morphometric characters. Measuring protocol is in Text-fig. 3.

side	Side of the ramus (left, right)
sr	Presence of the symphysial region (Y, N)
pst	Presence of parasymphisial teeth (Y, N)
tusk	Presence of the tusk (Y, N)
st	Site of the tusk (anterior, posterior, N)
er	Presence of an edentulous region (Y, N)
ao	Number of accessory openings (low, high)

Table 2. Categorical variables of morphometric characters.

one specimen of *C. intermedius* used as an outgroup (Text-fig. 3). The specimens differ not only in their general size but also in the proportions between the dimensions on the principal axes and in the form of the bones. In making all these measurements we have tried to quantify all the differences. The complete dataset is presented in Appendix 1.

The measurements have been taken with a digital calliper, except for the major lengths, which were taken with a meterstick. Some of them have been used to calculate the bend strength. Since the calliper measurements are in millimetres, with one decimal number, while the major lengths are in centimetres without decimals and generally greater than 10 cm, the data have been standardized. A Principal Component Analysis (PCA) was performed on the standardized dataset. A Shapiro-Wilk Test was performed to check the normality of data. K-means clusters have been added to the PCA plots and the plots of comparison between l2, w1, h3 and w3.

Some of these dimensions have been used to calculate the adaptation to stress according to beam theory. The simplified model of the ramus of the mandible is as a solid beam with an elliptical section. The axes of the ellipse are the labiolingual axis (*x*) and the dorsoventral axis (*y*) of the mandible (Text-fig. 2A). Then, the maximum force applied to any given point in the mandible is proportional to *Z* (the ratio of the section modulus of the mandibular corpus) /*L* (the distance of that point from the articular fossa). *Z/L* reveals variations in the magnitude of the applied force in different locations of the mandible and *Zx/Zy* is the relative mandibular strength in different planes. The mandibles that are deeper than wide (*Zx/Zy* > 1) are more adapted to resist dorsoventral loads, followed by sagittal bending; the ones that are wider than deep (*Zx/Zy* < 1) are adapted to resist labiolingual loads, followed by torsional stresses; the ones that are as deep as wide (*Zx/Zy* =1) are adapted to sustain both sagittal bending and torsional stresses (Hylander 1979). A complete mathematical explanation is provided in Appendix 2.

Concerning the ornamentation, 18 characters, modified from Witzmann *et al.* (2010), and Antczak and Bodzioch (2018), have been analysed (Table 3).

A Multiple Correspondence Analysis (MCA) was performed on these ornamentation data. All the statistics have been carried out with RStudio 2023.06.0+421.

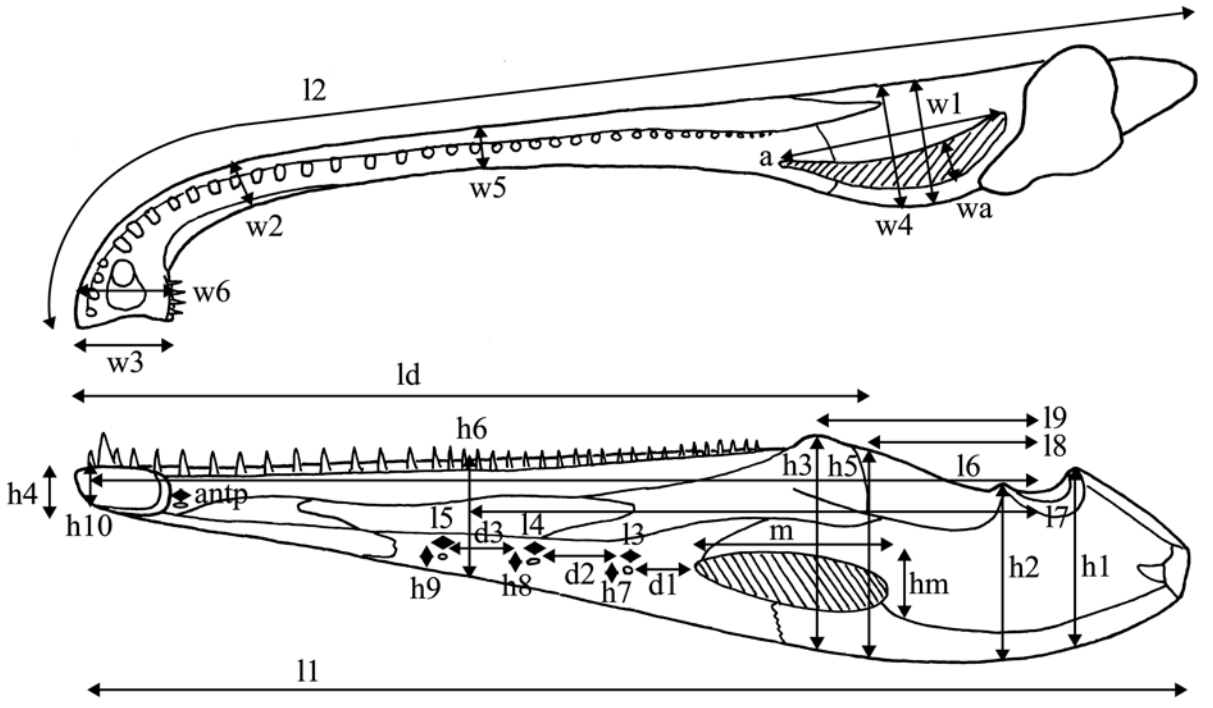

Text-fig. 3. Measuring protocol for measurements from Table 1 of the mandible in dorsal view, above, and lateral view on lingual side, below.

1	The ornamentation is regular (1); irregular (2)
2	The ridges are very sparse, i.e., <4 ridges in 2.5 cm in the vertical section at hamate and coronoid processes (1); sparse, 4–6 (2); dense, >6 (3)
3	Polygons are small, <5 mm (1); large, 5-6 mm (2); very large, >6 mm (3)
4	The height of the ridges is variable (1); mostly constant (2)
5	The ridges are deep, <3 mm (1); deep or shallow, 3-4 mm (2); shallow, >4 mm (3)
6	The height of the ridges is equal or slightly lower than the height of the nodal points (1); there are regions on which the height is the same and regions on which the ridges are lower (2); ridges are conspicuously lower than nodal points (3)
7	The width of the ridges is variable (1); mostly constant (2)
8	The ridges are fine, <2 mm (1); coarse, >2 mm (2)
9	The width of the ridges is at least half of the diameter of the appertaining cell (1); variable (2); narrower than the half of the diameter (3)
10	The nodal points are not broader or slightly broader than the ridges (1); distinctly broadened (2)
11	The ridges are broadly rounded dorsally (1); broadly rounded or narrow or edged dorsally (2); narrow or edged dorsally (3)
12	Sculptural cells constitute most of the sculptural pattern (1); radiating ridges and furrows constitute most of the sculptural pattern (2)
13	Sculptural cells are rather polygonal (1); polygonal or rounded (2); rather rounded (3)
14	The most common polygon are hexagons (1); pentagons (2); others (3)
15	Multipolygons are several or none (1); numerous (2)
16	No nodal points form tubercles (1); many nodal points form tubercles (2)
17	A deep furrow on the labial side of the dentary is absent (1); present (2)
18	A deep furrow on the lingual side of the angular is absent (1); present (2)

Table 3. Variables of ornamentation characters.

RESULTS

Morphometrics

Analysis of the PCA outputs (Text-fig. 4) indicates that the first PC represents only half of the variance and the variances of the four following PCs are still low. Only the first three PCs are taken into account herein, with 74% of the cumulative proportion of variance. PC1 is correlated to all the variables, in particular the ones related to the total and dentary length; PC2 shows a contrast between the lengths and the dimension of the openings; PC3 shows many contrasts between variables. In the plot of the PC1/PC2 scores, the best represented variables are the total length both along the longitudinal axis and along the labial margin, the length of the dentary, the width at the end of the dentary and in the middle of the dentary, and by the widths and the depths in the different sections along the longitudinal axis. All these variables are grouped along the *x* axis. In turn, on the *y* axis there are only dimensions of the third accessory opening in the postsplenial and the length of the first one, counting from the Meckelian window forward. This third opening is present only in two specimens, UOBS02062 and UOPB3490. Thus, it is possible to discriminate at least two groups along the *x* axis: the one on the right composed of specimens that lack a considerable part of the mandible and, as a consequence, have low length values, and the group in the middle with specimens that have an average length that increases toward the left. There are also two outgroups: UO2BP5V on the extreme left, which is *Cyclotosaurus*, considerably longer than *Metoposaurus*, and UOPB3490, which, despite its considerable length, has the third accessorial opening and is on the lower margin of the plot, while all the others are in the upper and middle parts. Considering that going from left to right, after UO2BP5V there are UOBS0323, the first longest metoposaur specimen, UOPB3503 and UOPB3504, the second and third longest specimens, UOBS02060, UOBS02061 and UOBS02062, that are also quite long, it shows that only the position of UOPB3490, the fourth longest specimen, is strongly affected by its particular character. Comparing PC1 and PC3, the variables on the *x* axis are the same, but with more emphasis on the heights, while the dimensions of the third accessorial opening are more grouped on the *y* axis. The pattern of the specimens is similar to that of the previous one, with the right and the central groups and UO2BP5V in the extreme left, but here the outgroup in the bottom is UOBS02062, the other specimen with the third accessory opening. All the other specimens are in the upper part of the plot. In PC2/PC3 there are three groups of variables: on the left of the *x* axis and upward, the dimensions of the openings in the lingual side and the heights and widths in the posterior part of the mandible; on the right part, and downward, the lengths and widths of the anterior part and the dentary and the distance between the dentary and the articulation; on the *y* axis, downward and

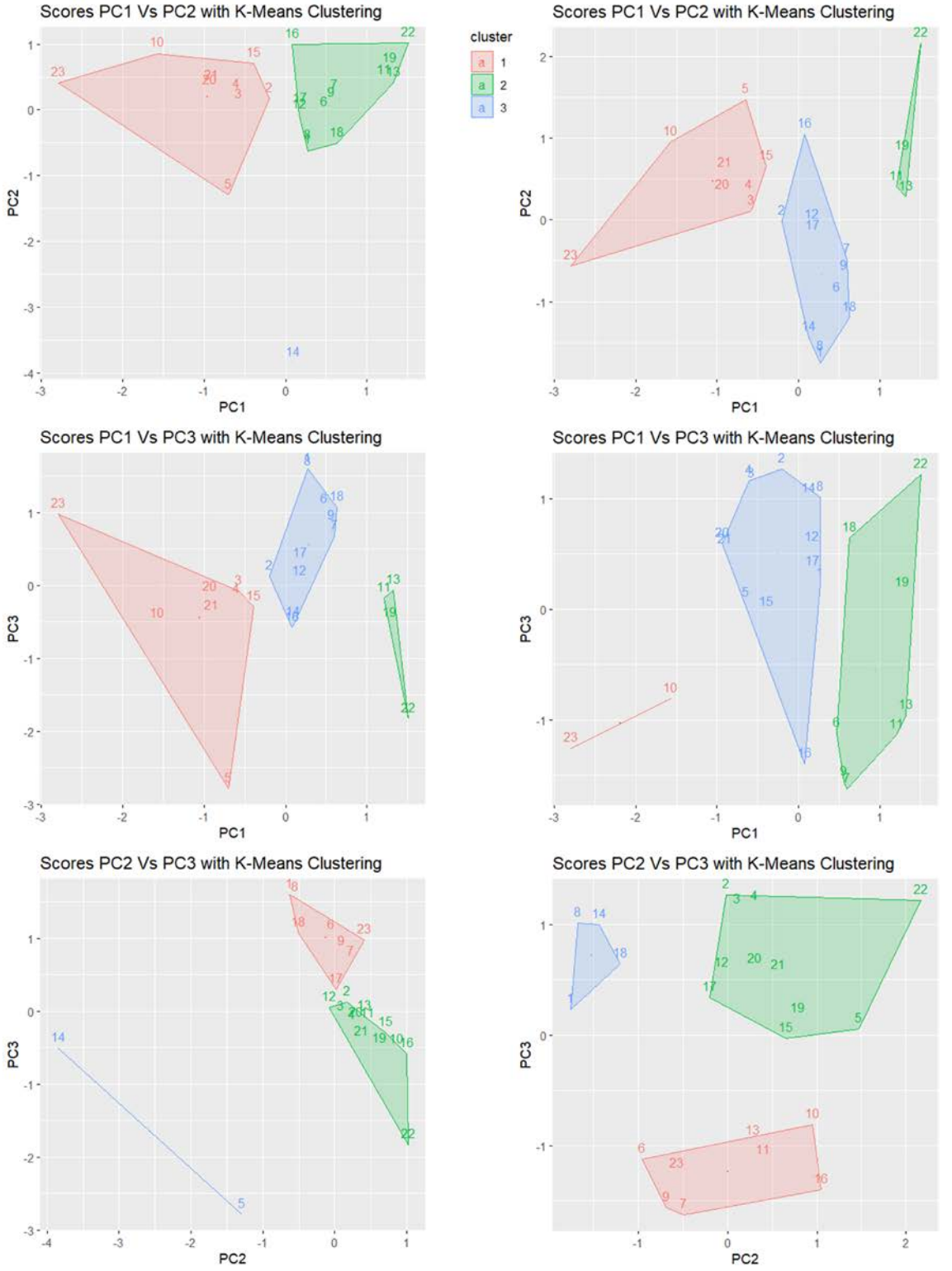

Text-fig. 4. PCA plots with k-means clustering: left column – with dimensions of 3rd accessory opening, dimensions for beam theory and incomplete specimens; right column – without. Specimens: 1 – UOBS01264; 2 – UOBS02059; 3 – UOBS02060; 4 – UOBS02061; 5 – UOBS02062; 6 – UOBS02063; 7 – UOBS02064; 8 – UOBS02065; 9 – UOBS02066; 10 – UOBS03023; 11 – UOPB3487; 12 – UOPB3488; 13 – UOPB3489; 14 – UOPB3490; 15 – UOPB3493; 16 – UOPB3494; 17 – UOPB3497; 18 – UOPB3498; 19 – UOPB3502; 20 – UOPB3503; 21 – UOPB3504; 22 – UOPB3505; 23 – UO2BP5V.

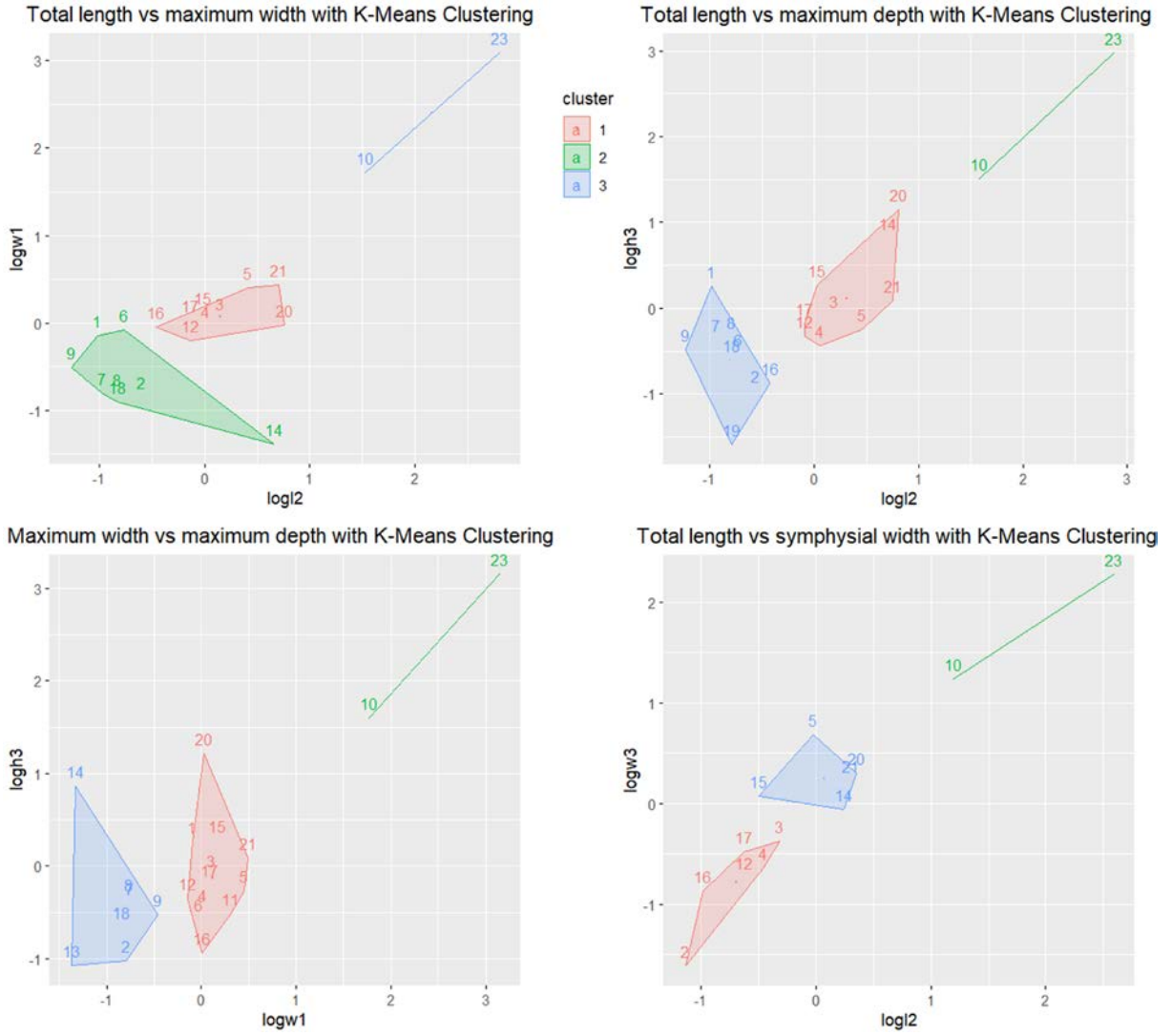

Text-fig. 5. Plots of the comparisons of total length, maximum depth and width, and width of the symphysial region after logarithmic transformation. Specimens: 1 – UOBS01264; 2 – UOBS02059; 3 – UOBS02060; 4 – UOBS02061; 5 – UOBS02062; 6 – UOBS02063; 7 – UOBS02064; 8 – UOBS02065; 9 – UOBS02066; 10 – UOBS03023; 11 – UOPB3487; 12 – UOPB3488; 13 – UOPB3489; 14 – UOPB3490; 15 – UOPB3493; 16 – UOPB3494; 17 – UOPB3497; 18 – UOPB3498; 19 – UOPB3502; 20 – UOPB3503; 21 – UOPB3504; 22 – UOPB3505; 23 – UO2BP5V.

leftward, again the dimension of the third accessory opening, but also the dimension of the symphysial region. There is a group of specimens in the top-right, but the outgroup on the left is UOPB3490 and the outgroup in the bottom is UOBS02062.

To balance the relationships between dimensions on different axes of the mandible corpus and avoid the situation that the exceptional characteristics of some specimens affect the result excessively, a new PCA was performed without the dimensions used for beam theory, which are directly proportional to the total length, the dimensions of the third accessorial opening, present on only two specimens, and the incomplete specimens (Text-fig. 4). The first three PCs represent 81% of the variance. This time in the case of PC1/PC2, UO2BP5V and UOBS03023 are in the top-left since they have the greater values of height and length, while the other specimens are grouped in the middle, with only the dimensions of the other openings on the lingual side closer to the negative *y* axis. In PC1/PC3, UOBS0323 is completely isolated in the bottom-left, and UOBS02060, UOBS02061, UOBS02062, UOPB3503 and UOPB3504 are distributed along the positive *y* axis. In PC2/PC3, to-

ward the bottom-right there are dimensions of the posterior and labial part, while toward top and left there are the dimensions of the openings on lingual side. The specimens are more scattered, with UOBS02062 in the top, UO2BP5V in the bottom, UOBS02059, UOBS02060 and UOBS02061 on the left and UOPB3488, UOPB3493 and UOPB3497 in the middle. Then, in general, the main contrasts are between the bones of the dorsal side and the bones of the ventrolingual side, and between the anterior part and the posterior part.

The distribution of total length along the labial margin, l2, the maximum width, w1, the maximum depth, h3, and the width of the symphysial region, w3, are not normal, even after logarithmic transformation, which is the most used transformation for this type of data. In all the distributions of these variables it is possible to discriminate a peak with small values composed of incomplete specimens, a larger group with a normal distribution, another group with larger specimens, UOBS02062, UOBS03023, UOPB3490, UOPB3503 and UOPB3504, and a last peak for the largest specimen, UO2BP5V. Nevertheless, the width and the depth have been compared with the length and with each other (Text-fig. 5). The result reflects what was already found with the PCA: besides the large and scattered group of small and incomplete specimens, similar ratios are shared by UOBS02061, UOBS02062, UOPB3490, UOPB3503, and UOPB3504, while UOBS03023 and UO2BP5V have greater values but follow the same trend.

Beam theory

The parameters regarding the adaptation to different types of loads have been calculated and plotted (Text-fig. 6). The mandible of *M. krasiejowensis* has, in general, a shallow profile with the articulation lower than the tooth row. The depth of the corpus increases from the symphysial region to the coronoid process. This determines an increase of *Zx/L* and *Zy/L* toward the posterior part of the corpus. The last two points in the plot do not reflect the actual shape of the mandible because the distances between the end of the dentary and articulation sometimes are lower than the distance between the section with the maximum depth. This occurs in specimens with a relatively high coronoid process. In *Cyclotosaurus*, instead, the hamate process is considerably high, and the dentary ends with a narrow and long line, while in *Metoposaurus* it decreases its depth rapidly, the maximum depth considered here is still the coronoid process in order to avoid differences in lengths between the two taxa. Nevertheless, it is possible, when analysing the plots, to distinguish three different patterns: in *Cyclotosaurus* the values in the mid-dentary, at the end of the dentary and in the highest depth are very different, and *Zx/Zy* is higher at the end of the dentary because here there is the hamate process, which is considerably higher than the rest of the corpus and, then, the *y* axis of the section is far higher than the *x* axis; the majority of *Metoposaurus* specimens have similar values of strength in the last two sections, because of the similar height of the processes, even if it is possible to identify slight differences between specimens with a large width and a relatively low coronoid process, e.g., UOBS02062, and specimens with a smaller width and a higher posterior part, e.g., UOPB3503; UOBS03023 has an intermediate feature between the two groups. Overall, the two taxa have always $Zx/Zy>1$, except for the symphysial region, which is flattened.

Other morphometric characters

Other morphometric characters have been evaluated as categorical data because of their features or the difficulty of being measured. An MCA was performed comparing the first three dimensions that represent 74% of the variance. In Dim1/Dim2 (Text-fig. 7A), the side of the mandibular corpus and the number of accessory openings are more represented on the *y* axis, while the tusk, the parasymphysial teeth, the symphysial region and the edentulous region are on the *x* axis. The position of the tusk is represented in the same way on both axes. It is possible to distinguish two groups along the *y* axis: specimens, especially UOPB3503, UOPB3504 and UOBS0323, with the left side and anterior tusk, and specimens, such as UOBS02059, UOBS02060, UOBS02061, UOBS02062, with the right side and posterior tusk. On the *x* axis, instead, the contrast mainly concerns the presence or absence of tusk or teeth and thus, it reflects more the preservation of the sample than osteological features, except for the number of accessory openings. Dim1/Dim3 and Dim2/Dim3 accentuate, respectively, the contrasts on the *x* and *y* axes.

Ornamentation

MCA was also performed with categorical data concerning the ornamentation (Text-fig. 7B). In Dim1/Dim2, the *y* axis represents mainly the variables about the depth of the ridges, while the *x* axis is the shape of the polygons. All the specimens are grouped around the origin of axes, except for UO2BP5V in the upper part and UOBS02060 in the top-right. In

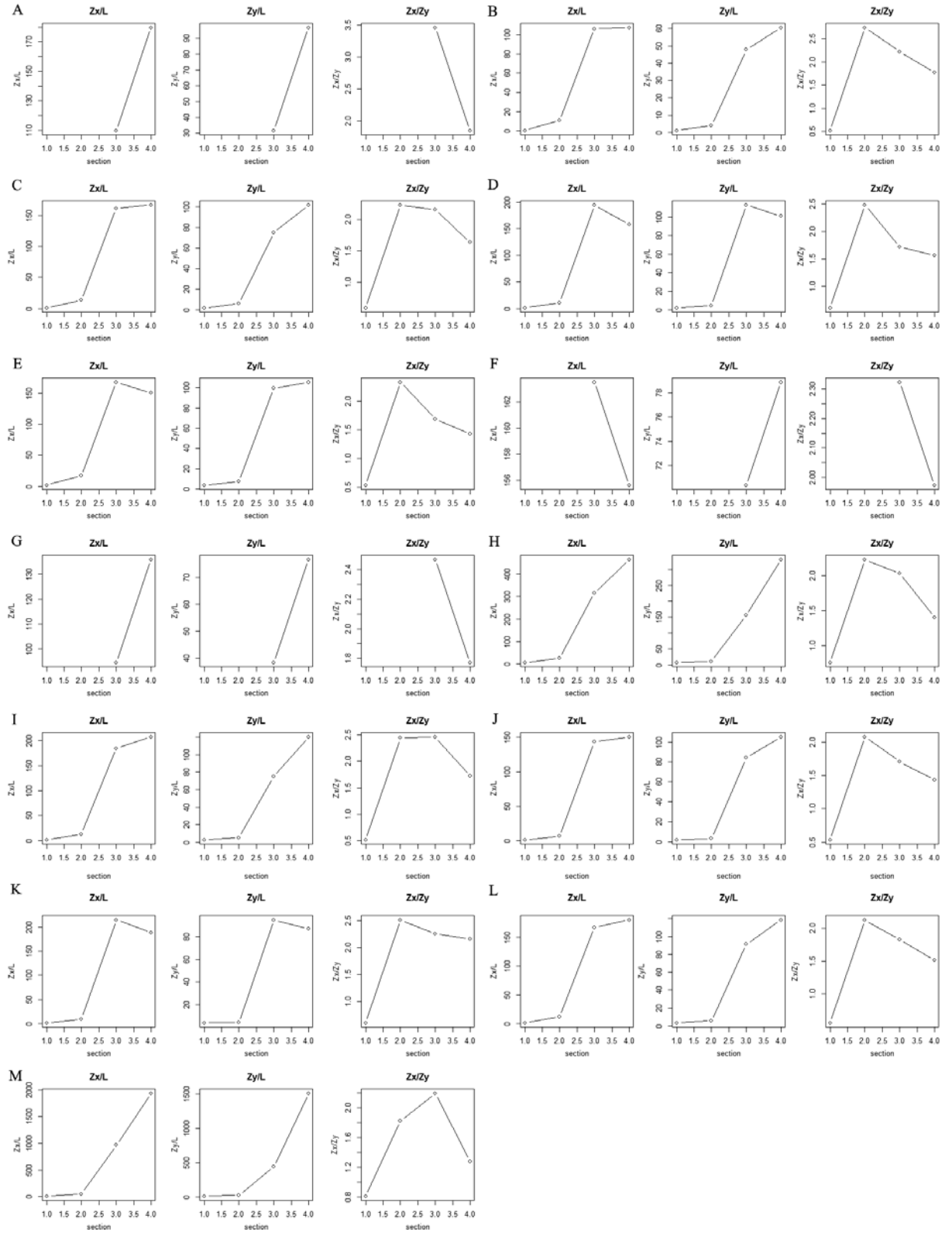

Text-fig. 6: Plots of the bending strength in: A – UOBS01264; B – UOBS02059; C – UOBS02060; D – UOBS02061; E – UOBS02062; F – UOBS02064; G – UOBS02066; H – UOBS03023; I – UOPB3493; J – UOPB3494; K – UOPB3503; L – UOPB3504; M – UO2BP5V.

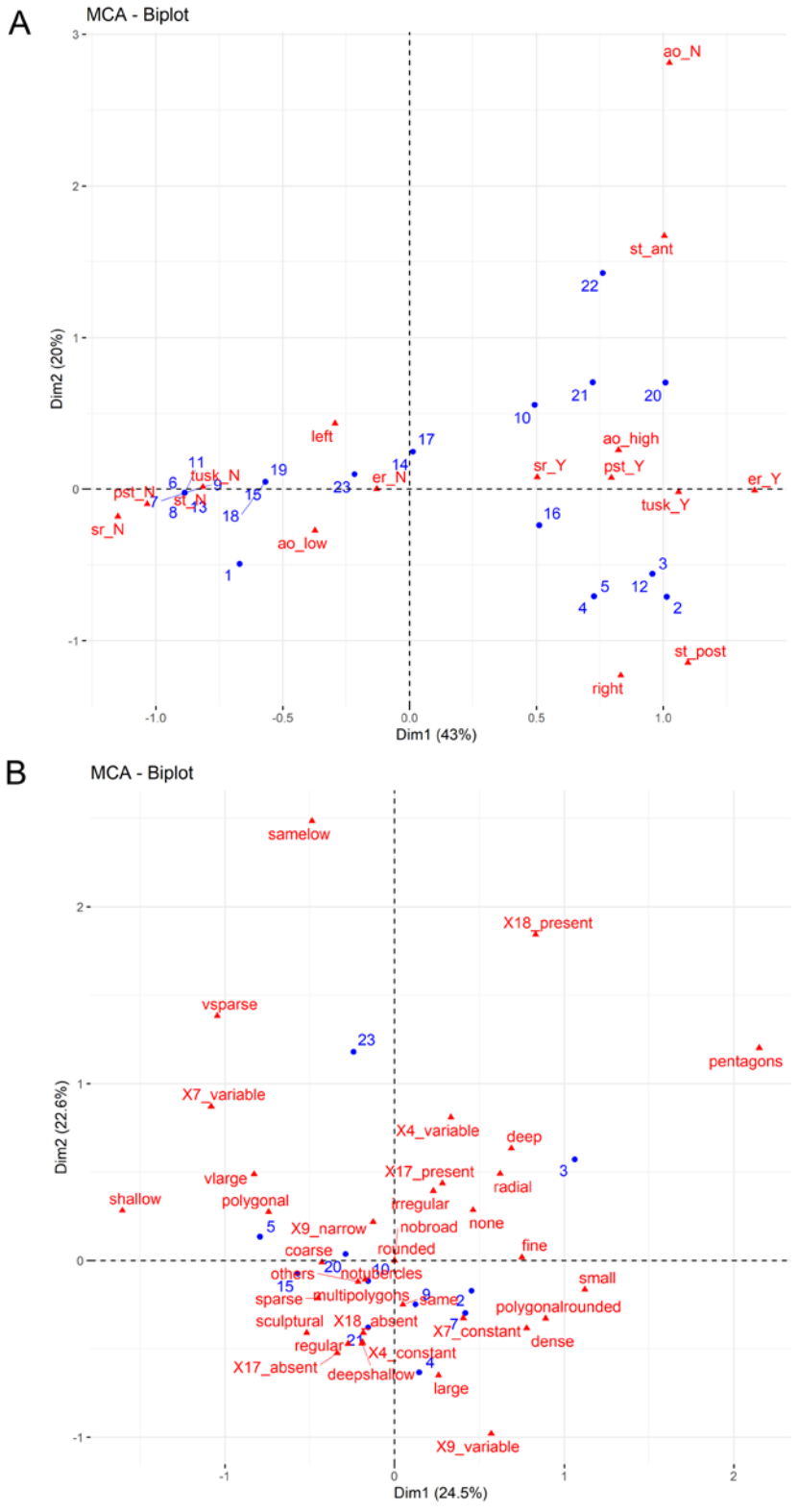

Text-fig. 7. MCA plot of: A – Categorical variables of morphometrics characters; B – Dermal bone ornamentation characters. Specimens: 1 – UOBS01264; 2 – UOBS02059; 3 – UOBS02060; 4 – UOBS02061; 5 – UOBS02062; 6 – UOBS02063; 7 – UOBS02064; 8 – UOBS02065; 9 – UOBS02066; 10 – UOBS03023; 11 – UOPB3487; 12 – UOPB3488; 13 – UOPB3489; 14 – UOPB3490; 15 – UOPB3493; 16 – UOPB3494; 17 – UOPB3497; 18 – UOPB3498; 19 – UOPB3502; 20 – UOPB3503; 21 – UOPB3504; 22 – UOPB3505; 23 – UO2BP5V.

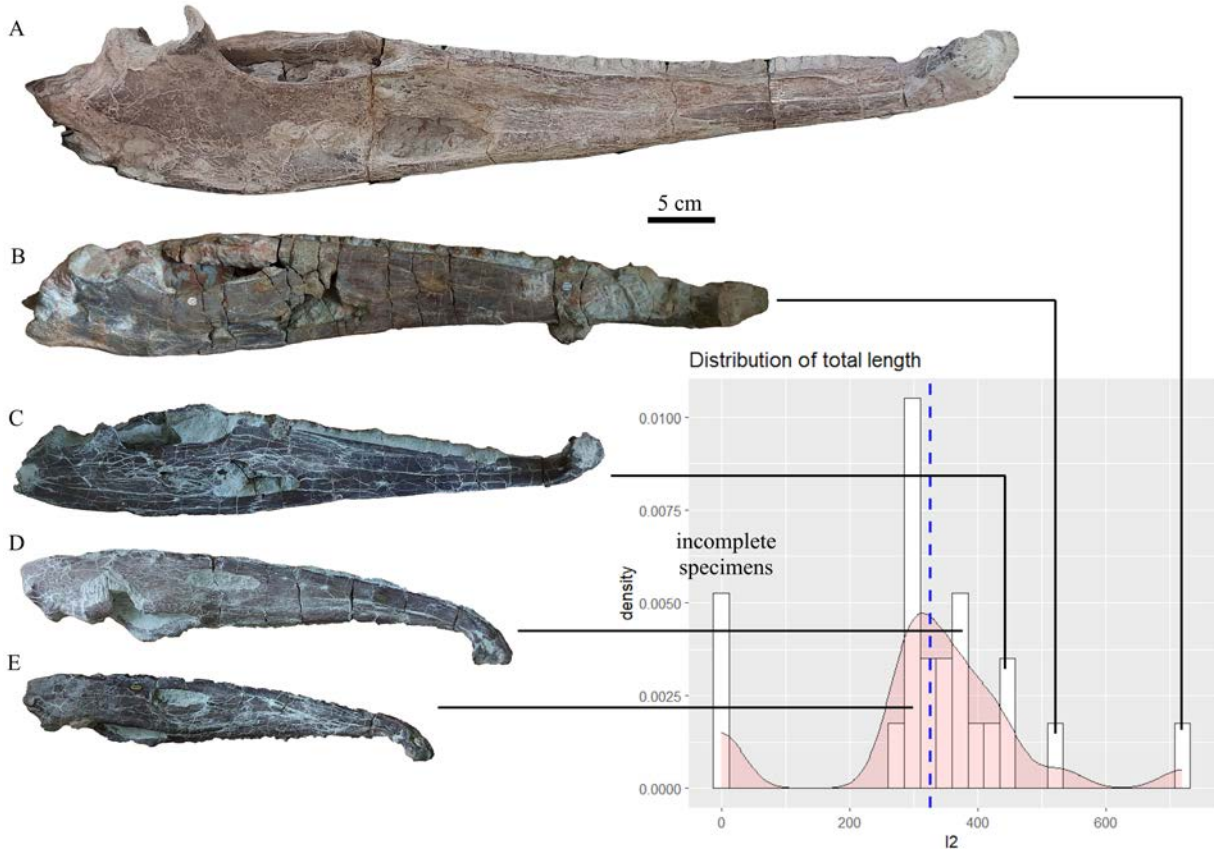

Text-fig. 8. Distribution of total length along the labial size of the mandible of *Metoposaurus krasiejowensis* Sulej, 2002 and most representative specimens: A – UO2BP5V (*Cyclotosaurus intermedius* Sulej and Majer, 2005); B – UOBS03023; C – UOPB3503; D – UOBS02060 and E – UOBS02059.

Dim1/Dim3 and Dim2/Dim3 the specimens are quite scattered, generally with larger specimens around the origin. However, it is possible to draw a contrast between *Metoposaurus* and *Cyclotosaurus* in the width and depth of ridges.

DISCUSSION

Despite the high number of measured morphometric characters, the majority of variables are grouped and, as a consequence, only a few of them are significant. First of all, the PCA results show a contrast between the features of the dentary and the bones on the lingual side, the latter being more variable. This makes it more difficult to recognize overall similarities between different specimens. However, it is possible to group the specimens with two criteria. The total length is the dimension that mostly affects the result and, besides incomplete specimens and *Cyclotosaurus*, at least three groups of specimens each with very similar sizes can be distinguished. The simplest explanation is that the majority of specimens belong to juvenile or early adult individuals, e.g., UOBS02059, UOBS02060 and UOBS02061, while the larger specimens, UOBS02062 and UOPB3493, represent old individuals. Very young individuals are absent (Antczak and Bodzioch 2018), while the exceptionally old adult could be represented by the few largest specimens, UOPB3490, UOPB3503, UOPB3504 and UOBS03023. The last group actually constitutes two peaks in the distribution, which thus is not normal (Text-fig. 8). It is difficult to estimate how much the distribution of mandible sizes represents the actual distribution. Catastrophic flood events might have transported the carcasses and deposited them together in what today is the Krasiejów site (Bodzioch and Kowal-Linka 2012) or even be responsible for the death of all the individuals (Konietzko-Meier and Klein 2013). In this case, the distribution might be completely random or affected by the size of the bone itself, since the small bones of vertebrates have a higher probability of being damaged or destroyed

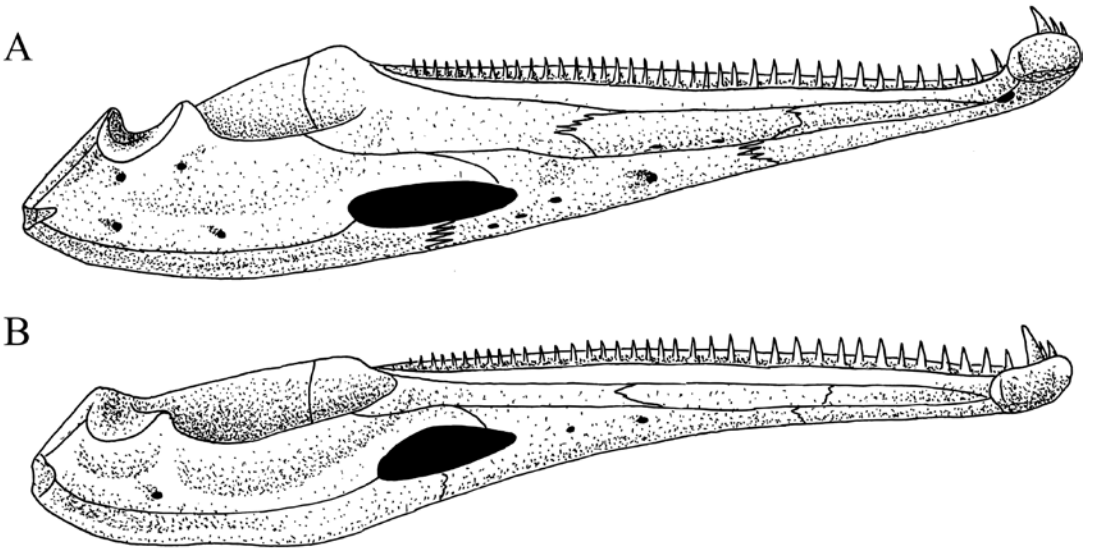

Text-fig. 9. Representation of type 1 (A) and type 2 (B) of the mandible of *Metoposaurus krasiejowensis* Sulej, 2002, slightly exaggerating the morphological differences (curvature of the corpus, shape of Meckelian window, number of accessory openings, height of coronoid process).

during taphonomic processes (Brown *et al.* 2013) and, indeed, here the most incomplete specimens are the smallest ones. Not even the ontogenetic age can be precisely established with skeletochronological data, unlike the case with long bones (Konietzko-Meier and Sander 2013; Gruntmejer *et al.* 2021).

Considering the dimensions as a whole, instead, the PCA groups the specimens in three sets. The sets are not always the same, but considering the trajectories in the plots of the length, depth and width ratios, the greatest distances in MCA and PCA, being aware of the influence of the dimensions along the longitudinal axis, the division into three groups seems the most plausible. Specimens UOBS02059, UOBS02060, UOPB3490, UOBS02065 and UOPB3503 have a relatively high coronoid process and a generally large depth compared to the width, a narrow adductor fossa, numerous accessory openings and pits, the number of which increases with the increase of size, and a long longitudinal ridge on the anterolabial side. For the sake of simplicity, this group is indicated as type 1 (Text-fig. 9A). Type 2 (Text-fig. 9B) in turn, composed of UOBS02061, UOBS02062, UOPB3493 and UOPB3504, presents a higher width, an almost constant depth in the area near the coronoid process, a gentle decrease of depth toward the anterior part, a reduced and even bottomward curvature of the corpus and less accessory openings. The other specimens are similar to both UOBS02059 and UOBS02061. This means that, if the small specimens represent young individuals, the greater diversity occurs in adults. The third group is actually the outgroup, the *Cyclotosaurus* specimen UO2BP5V, but UOBS03023 often presents intermediate characteristics between type 2 and the outgroup.

Ecological implications of the morphology and ornamentation variations

Assuming that the groups in the size distribution represent at least three ontogenetic stages, the differences between type 1 and 2 require a different explanation. Besides morphological differences, type 1 presents a more polygonal, dense and thin ornamentation, while type 2 a more radial and sparse ornamentation with more robust ridges. These differences could be indicative of a more aquatic lifestyle for type 1 and more terrestrial for type 2. However, it is not possible to find a strong correspondence between the two types of ornamentation, and the typical aquatic and terrestrial ornamentations, as in other studies concerning above all the ornamentation of the skull and girdle (Witzmann *et al.* 2010; Antczak and Bodzioch 2018).

The two habitats would be not completely aquatic or terrestrial but aquatic and semiterrestrial. Even if the lifestyle of *Metoposaurus* and other stereospondyls is considered aquatic, at least in the adult form, because of the presence of the lateral line and small limbs (Lucas *et al*. 2016; Rinehart and Lucas 2016), this does not mean that these animals cannot present some adaptations to a semiterrestrial environment. The large manus of *M. krasiejowensis* with a relatively

Text-fig. 10. Main differences between larger specimens of the mandible of *Metoposaurus krasiejowensis* Sulej, 2002. A – Anterior tusk with edentulous region in left side in UOPB3503; B – Posterior tusk without edentulous region in right side in UOBS02062; C – absence of tusk in UOPB 3497; D – Narrow adductor fossa in UOPB3503; E – Large adductor fossa in UOPB3504; F – Large adductor fossa in UOBS03023; G – Adductor fossa in UO2BP5V; H – Numerous accessory openings in UOPB3503.

short and wide humerus possibly enabled it to burrow underground during the long unfavourable part of the year (Konietzko-Meier and Sander 2013), instead ofmaking it able to swim with four limbs, as previously believed (Sulej 2007). So, propulsion was generated by the tail and the animal could have lived in water shallow enough to easily reach the bottom, to burrow in it and to make an ambush, as suggested by the mechanical features of the skull that could have allowed the animal to capture prey by both lateral and bilateral bites during active swimming, but also remaining buried in mud and attacking by ambush (Konietzko-Meier *et al.* 2018; Gruntmejer *et al.* 2019b).

The morphology of the humeri indicates a uniform bone growth represented by only one morphotype, while the femora shows a bimodal morphological distribution (Teschner *et al.* 2018). In addition, histological analysis indicates the presence of two histotypes: the former is characterized by fast growth and fast remodelling, and the latter by alternating phases of slowed growth (Teschner *et al.* 2018). The reason of the presence for different histotypes and different ecotypes could be ecological. Different layers in the long bones (Konietzko-Meier and Sander 2013), found also in teeth (Weryński and Kędzierski 2022), representing a cyclical pattern of growth, indi-

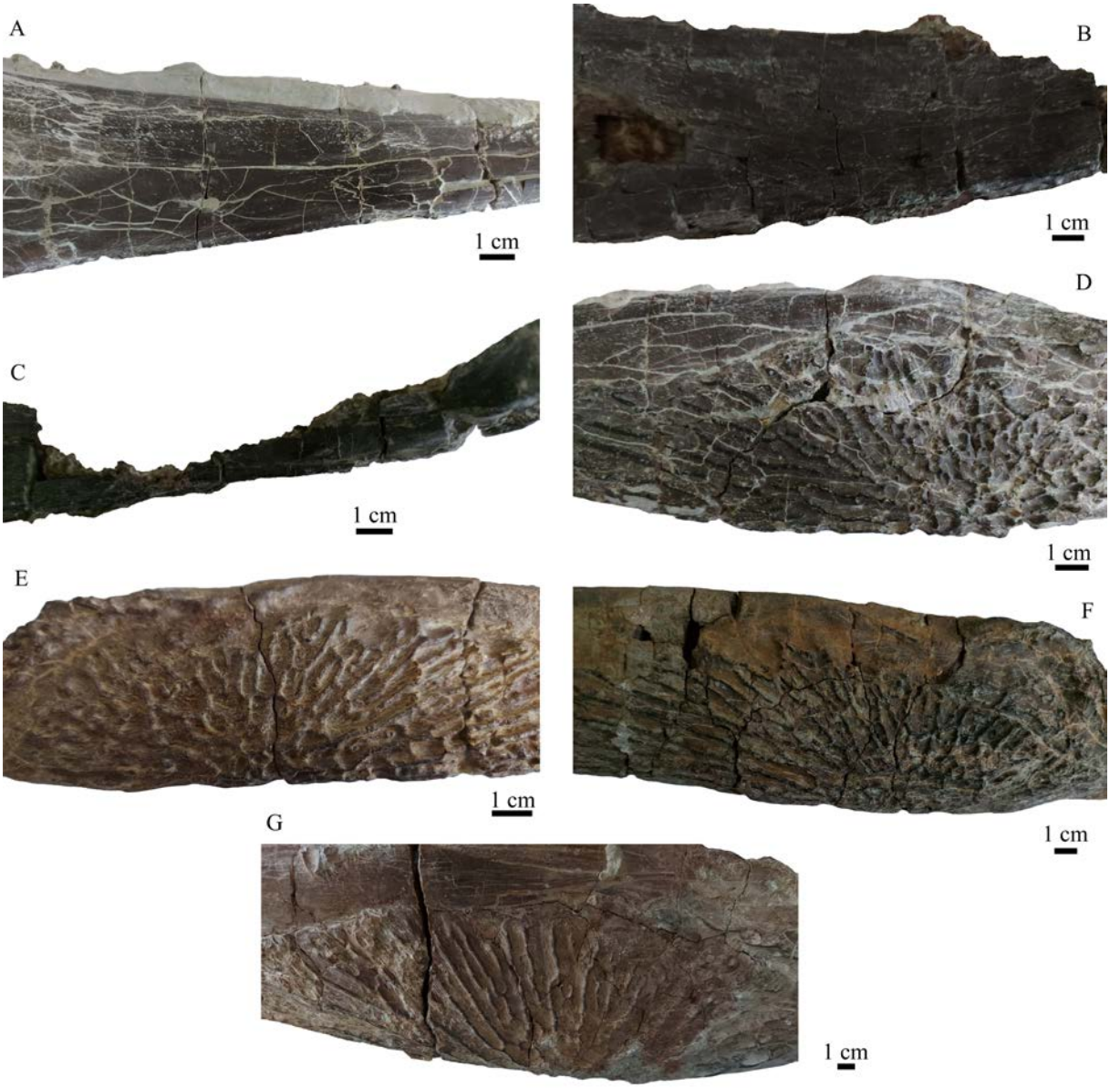

Text-fig. 11. Main differences between larger specimens of the mandible of *Metoposaurus krasiejowensis* Sulej, 2002. A – accessory openings in intercoronoid in UOPB3503; B – three accessory openings in postsplenial in UOPB3490; C – accessory opening in splenial in UOPB3490; D – ornamentation in angular in UOPB3503; E – ornamentation in angular in UOBS02061; F – ornamentation in angular in UOBS03023; G – ornamentation in angular in UO2BP5V.

cate an alternation of dry periods and heavy rainfalls (Bodzioch and Kowal-Linka 2012). Thus, *M. krasiejowensis* might have been able to adapt its ontogenetic trajectory in response to ecological changes, even if terrestrialization as a phase of an ecologically-controlled metamorphosis has been observed in eryopoids and in the Permo-Carboniferous sterespondylomorph *Sclerocephalus haeuseri* Goldfuss, 1847, more than in Triassic sterospondyls (Schoch 2009a, b, 2010).

Feeding mechanics

The shape of sutures in the symphysial region and at the contact between the angular, surangular and prearticular indicates a tensile stress in these areas, probably due to a great gape during predation (Gruntmejer *et al.* 2019a). The results of the beam theory applied to the mandible in the present work confirm that the mandible could support dorsoventral

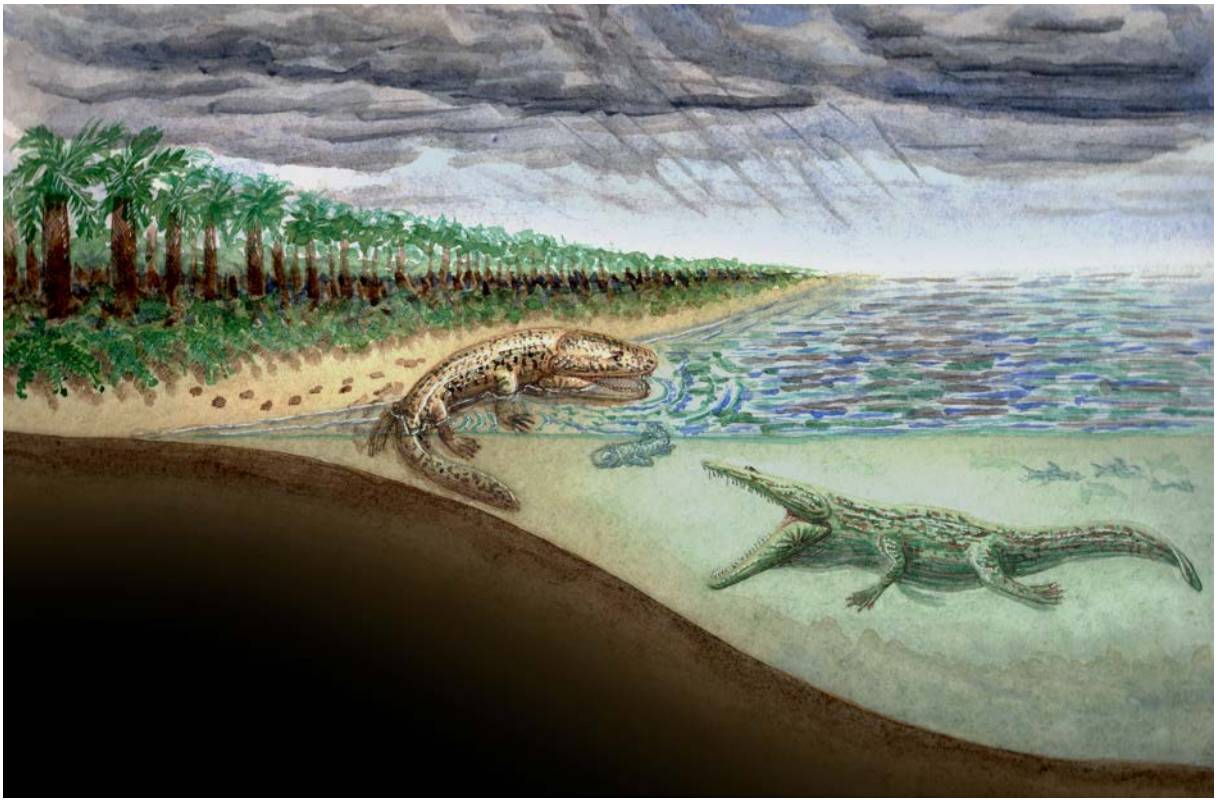

Text-fig. 12. Paleoartistic representation of two individuals of *Metoposaurus krasiejowensis* Sulej, 2002 hunting the same prey but in different ways: one generating a propulsion with tail in shallow water and trying to swallow the prey (active hunting in fully aquatic environment), the other one trying to bite it with an unexpected, rapid and lateral movement (ambush in semiterrestrial environment).

loads with a wide and rapid bite. Applying the beam theory to a single tooth, instead, indicates that temnospondyl teeth are labiolingually elongated at the base and circular in cross-section at some distance above the base in order to better support labiolingual loads (Rinehart and Lucas 2013b). So, the mandible presents different ways to adapt to different loads. This makes possible a crocodile-like lifestyle for *M. krasiejowensis* and similar species, including *C. intermedius*, even if crocodiles have a more powerful bite and can hold the prey at the end of the bite. The mandible of crocodiles and other apex predators, e.g., theropod dinosaurs, with similar feeding habits, is in fact more robust in both anterior and posterior extremities (Therrien *et al.* 2005). In *M. krasiejowensis* instead, the symphysial region is horizontally flattened. On the other hand, it has a lower porosity than the rest of the mandible, which could be an adaptation to stress (Gruntmejer *et al.* 2021). A FEA of the skull of *Cyclotosaurus* and other capitosaurs confirms the hypothesis that these species had the ability to hunt larger prey and had generalist, crocodile-like feeding habits (Fortuny *et al.* 2012). A morphometric analysis based only on the width/length ratio of the rostrum, instead, collocates the temnospondyls between the brevirostrine species of extant salamanders and longirostrine species of phytosaurs and crocodiles (Rinehart et al. 2023). Thus, the analysis of the mandibular force profile performed in the present work, rather than showing a relevant difference between the two groups, confirms the conclusion that the type and size of the prey items, and the hunting techniques, from ambush to active hunting, were highly variable among temnospondyls, and in particular among metoposaurids and capitosaurs.

Possible sexual dimorphism

Since there are two morphological groups, a possible explanation could be sexual dimorphism. Not much is known about the sexual features and mating behaviour among the Temnospondyli, except for a hypothesis of internal fertilization suggested by the preservation of three body impressions of temnospondyls

from the Mississippian of eastern Pennsylvania, USA (Lucas *et al.* 2010). It is possible to make comparisons with the cryptobranchids, i.e., giant salamanders in which species females are generally larger than males (Shine 1979), and parental care behaviours have been described (Settle *et al.* 2018; Vági *et al.* 2022). Other features that have been attributed to sexual dimorphism are the angle of the skull and other characteristics of the girdle and pelvic bones, the distributions of which are bimodal in some temnospondyl species, including *M. krasiejowensis* and *Koskinonodon perfectus* Case, 1922 (Rinehart and Lucas 2023). In addition, in *Koskinonodon*, a lower skull angle is associated with higher values of the skull length (Rinehart *et al.* 2023). The ratio between specimens of the two types in the present work (about 1:1) are compatible with the sex ratio in living species, 1.4:1 m/f (Rinehart and Lucas 2023), making possible the attribution of the morphological differences to sexual dimorphism, even if the distinction between the two types is based on numerous characters and is not so clear. Moreover, this does not exclude ecological adaptation, sexual dimorphism only remaining more speculative.

Unsolved questions

The function of the accessory openings is not clear and it is noteworthy that little foramina have been found horizontally aligned in the intercoronoid of UOPB3503, but vertically in *M. algarvensis* (Brusatte *et al.* 2015). Analogously, it is not possible at the moment to find an explanation for the presence of an edentulous region in two specimens, UOBS02059 and UOPB3503, also found in *M. algarvensis* (Brusatte *et al.* 2015), the absence of the tusk not due to taphonomic reasons in UOPB3497, and the strong correlation between the anterior position of the tusk, and the left side of the mandible and the posterior position with the right side. Maybe finds of other specimens in the future will help to clarify these aspects.

CONCLUSIONS

Measuring and analysing the morphological characters of the mandible of *M. krasiejowensis* has not only added numerous details to previous descriptions (Sulej 2002, 2007) but has revealed interesting new palaeoecological information. Besides the fact that the main difference between the specimens is the length, and that the increase of width and depth seems to be allometric, the differences between the largest specimens regarding their dimensions without a normal distribution, the number of accessory openings and the dermal ornamentation (Text-figs 10 and 11) have been interpreted as adaptations to different lifestyles, aquatic and semiterrestrial (Text-fig. 12). Other authors have found evidence of different habits among populations of *M. krasiejowensis* in histology (Teschner *et al.* 2018) and ornamentation (Antczak and Bodzioch 2018) and the present work adds another argument in this direction. Numerous other specimens in Opole have not been considered herein because their preparation would be long and dangerous. In the future, comparing all these specimens with others found in the bone bed in Krasiejów and those kept in the collection of the Polish Academy of Sciences in Warsaw, will allow us to have a better understanding of the intraspecific variation of this species, and as a consequence, a better understanding of the fluvial environment of the Late Triassic, in relation to a common and diversified vertebrate group such as the Temnospondyli.

Acknowledgements

We thank the reviewers Spencer Lucas and Dorota Konietzko-Meier and the editor Anna Żylińska for helpful comments that improved the manuscript.

REFERENCES

Ahlberg, P.E. and Clack, J.A. 1998. Lower jaws, lower tetrapods – a review based on the Devonian genus *Acanthostega*. *Transactions of the Royal Society of Edinburgh: Earth Sciences*, **89** (1), 11–46.

Anderson, P.S.L., Friedman, M. and Ruta, M. 2013. Late to the table: diversification of tetrapod mandibular biomechanics lagged behind the evolution of terrestriality. *Integrative and Comparative Biology*, **53** (2), 197–208.

Antczak, M. and Bodzioch, A. 2018. Ornamentation of dermal bones of *Metoposaurus krasiejowensis* and its ecological implications. *PeerJ*, **6**, e5267.

Barycka, E. 2007. Morphology and ontogeny of the humerus of the Triassic temnospondyl amphibian Metoposaurus diagnosticus. *Neues Jahrbuch für Geologie und Paläontologie, Abhandlungen*, **243** (3), 351–361.

Biewener, A.A. 1992. Overview of structural mechanics. In: Biewener, A.A. (Ed.), Biomechanics, Structures and Systems: A Practical Approach, 1–20. Oxford University Press; Oxford.

Biknevicius, A.R. and Ruff, C.B. 1992. The structure of the mandibular corpus and its relationship to feeding behaviours in extant carnivorans. *Journal of Zoology*, **228** (3), 479–507.

Bilan, W. 1975. The Rhaetic profile in Krasiejów near Opole. *Geologia*, **1** (3), 13–19.

Bodzioch, A. and Kowal-Linka, M. 2012. Unraveling the origin

of the Late Triassic multitaxic bone accumulation at Krasiejów (S Poland) by diagenetic analysis. *Palaeogeography, Palaeoclimatology, Palaeoecology*, **346**–**347**, 25–36.

Boy, J.A. and Sues, H.D. 2000. Branchiosaurs: Larvae, Metamorphosis and Heterochrony in Temnospondyls and Seymouriamorphs. In: Heatwole, H. and Carroll, R.L. (Ed.), Amphibian Biology 4. Palaeontology, 1150–1197. Surrey Beatty; Chipping Norton.

Brown, C.M., Evans, D.C., Campione, N.E., O'Brien, L.J. and Eberth, D.A. 2013. Evidence for taphonomic size bias in the Dinosaur Park Formation (Campanian, Alberta), a model Mesozoic terrestrial alluvial-paralic system. *Palaeogeography, Palaeoclimatology, Palaeoecology*, **372**, 108–122.

Brusatte, S.L., Butler, R.J., Mateus, O. and Steyer, J.S. 2015. A new species of *Metoposaurus* from the Late Triassic of Portugal and comments on the systematics and biogeography of metoposaurid temnospondyls. *Journal of Vertebrate Paleontology*, **35** (3), e912988.

Brusatte, S.L., Butler, R.J., Sulej, T. and Niedźwiedzki, G., 2009. The Taxonomy and Anatomy of Rauisuchian Archosaurs from the Late Triassic of Germany and Poland. *Acta Palaeontologica Polonica*, **54** (2), 221–230.

Busbey, A.B. 1995. Structural consequences of skull flattening in crocodilians. In: Thomason, J.J. (Ed.), Functional Morphology in Vertebrate Paleontology, 173–192. Cambridge University Press; Cambridge.

Bystrow, A.P. 1935. Morphologische Untersuchungen der Deckknochen des Schädel der WirbelTiere. I-Mitteilung: Schädel der Stegocephalen. *Acta Zoologica*, **16** (1–2), 65–141.

Bystrow, A.P. 1947. Hydrophilous and xerophilous labyrinthodonts. *Acta Zoologica*, **28** (1), 137–164.

Case, E.C., 1922. New reptiles and stegocephalians from the Upper Triassic of western Texas. In: Case, E.C. (Ed.), 120 pp. Carnegie Institution of Washington; Washington.

Christiansen, P. and Adolfssen, J.S. 2005. Bite forces, canine strength and skull allometry in carnivores (Mammalia, Carnivora). *Journal of Zoology*, **266** (2), 133–151.

Christiansen, P. and Wroe, S. 2007. Bite forces and evolutionary adaptations to feeding ecology in carnivores. *Ecology*, **88** (2), 347–358.

Clack, J.A., Ahlberg, P.E., Blom, H. and Finney, S.M. 2012. A new genus of Devonian tetrapod from North-East Greenland, with new information on the lower jaw of *Ichthyostega*. *Palaeontology*, **55**, 73–86.

Clarac, F., Souter, T., Cornette, R., Cubo, J. and De Buffrénil, V. 2015. A quantitative assessment of bone area increase due to ornamentation in the Crocodylia. *Journal of Morphology*, **276** (10), 1183–1192.

Coldiron, R.W. 1974. Possible functions of ornament in labyrinthodont amphibians. *Occasional Papers of the Museum of Natural History of Lawrence*, **33**, 1–19.

Cosgriff, J.W. and Zawiskie, J.M. 1979. A new species of the Rhytidosteidae from the Lystrosaurus zone and a review of the Rhytidosteoidea. *Palaeontologica Africana*, **22**, 1–27.

Credner, H. 1881. Die Stegocephalen aus dem Rothliegenden des Plauen'schen Grundes bei Dresden. *Zeitschrift der Deutschen Geologischen Gesellschaft*, **33** (4), 574–603.

Cuff, A.R. and Rayfield, E.J. 2013. Feeding mechanics in spinosaurid theropods and extant crocodilians. *PLoS ONE*, **8** (5), e65295.

Daeschler, E.B., Shubin, N.H. and Jenkins, F.A. 2006. A Devonian tetrapod-like fish and the evolution of the tetrapod body plan. *Nature*, **440** (7085), 757–763.

De Buffrénil, V. 1982. Morphogenesis of bone ornamentation in extant and extinct crocodilians. *Zoomorphology*, **99** (2), 155–166.

De Buffrénil, V., Clarac, F., Fau, M., Martin, S., Martin, B., Pellé, E. and Laurin, M. 2015. Differentiation and growth of bone ornamentation in vertebrates: A comparative histological study among the Crocodylomorpha: development of bone ornamentation in the Crocodylomorpha. *Journal of Morphology*, **276** (4), 425–445.

De Buffrénil, V., Dauphin, Y., Rage, J.-C. and Sire, J.-Y. 2011. An enamel-like tissue, osteodermine, on the osteoderms of a fossil anguid (Glyptosaurinae) lizard. *Comptes Rendus Palevol*, **10** (5–6), 427–437.

Dias, E.V. and Richter, M. 2002. On the squamation of Australerpeton cosgriffi Barberena, a temnospondyl amphibian from the Upper Permian of Brazil. *Anais da Academia Brasileira de Ciências*, **74** (3), 477–490.

Dzik, J. 2001. A new Paleorhinus fauna in the early Late Triassic of Poland. *Journal of Vertebrate Paleontology*, **21**, 625–627.

Dzik, J. 2003. A breaked herbivorous Archosaur with dinosaur affinities from the early Late Triassic of Poland. *Journal of Vertebrate Paleontology*, **23**, 556–574.

Dzik, J. and Sulej, T. 2007. A review of the early Late Triassic Krasiejów biota from Silesia, Poland. *Palaeontologia Polonica*, **64**, 3–27.

Figueirido, B., Tseng, Z.J., Serrano-Alarcón, F.J., Martín-Serra, A. and Pastor, J.F. 2014. Three-dimensional computer simulations of feeding behaviour in red and giant pandas relate skull biomechanics with dietary niche partitioning. *Biology Letters*, **10** (4), 20140196.

Fijałkowska-Mader, A. 2015. Record of climatic changes in the Triassic palynological spectra from Poland. *Geological Quarterly*, **59**, 615–653.

Fortuny, J., Marcé-Nogué, J., Gil, L. and Galobart, À. 2012. Skull mechanics and the evolutionary patterns of the otic notch closure in capitosaurs (Amphibia: Temnospondyli). *The Anatomical Record: Advances in Integrative Anatomy and Evolutionary Biology*, **295** (7), 1134–1146.

Fraas, E. 1889. Die Labyrinthodonten der schwäbischen Trias. *Palaeontographica*, **36** (1–3), 1–158.

Fritsch, A. 1889. Fauna der Gaskohle und der Kalksteine der Permformation Böhmens, Vol. 2, 92 pp. Selbstverlag; Prag.

Fry, B.G., Wroe, S., Teeuwisse, W., Van Osch, M.J.P., Moreno, K., Ingle, J., McHenry, C., Ferrara, T., Clausen, P., Scheib, H., Winter, K.L., Greisman, L., Roelants, K., Van Der Weerd, L., Clemente, C.J., Giannakis, E., Hodgson, W.C., Luz, S., Martelli, P., Krishnasamy, K., Kochva, E., Kwok, H.F., Scanlon, D., Karas, J., Citron, D.M., Goldstein, E.J.C., Mcnaughtan, J.E. and Norman, J.A. 2009. A central role for venom in predation by *Varanus komodoensis* (Komodo Dragon) and the extinct giant *Varanus* (*Megalania*) *priscus*. *Proceedings of the National Academy of Sciences*, **106** (22), 8969–8974.

Giles, S., Rücklin, M. and Donoghue, P.C.J. 2013. Histology of "placoderm" dermal skeletons: Implications for the nature of the ancestral gnathostome. *Journal of Morphology*, **274** (6), 627–644.

Goldfuss, A., 1847. Beiträge zur vorweltlichen Fauna des Steinkohlengebirges. 27 pp. Naturhistorischer Verein der Preussischen Rheinlande; Bonn.

Grodzicka-Szymanko, W. 1971. Cyclic-sedimentary subdivision of the Rhaetian of the Polish Lowlands. *Bulletin de l'Académie Polonaise des Sciences, série des Sciences de la Terre*, **19**, 137–147.

Gross, W. 1941. Über den Unterkiefer einiger devonischer Crossopterygier. *Abhandlungen der Preussischen Akademie der Wissenschaften, Mathematisch-Naturwissenschaftliche Klasse*, **7**, 1–51.

Gruntmejer, K., Bodzioch, A. and Konietzko-Meier, D. 2021. Mandible histology in *Metoposaurus krasiejowensis* (Temnospondyli, Stereospondyli) from the Upper Triassic of Poland. *PeerJ*, **9**, e12218.

Gruntmejer, K., Konietzko-Meier, D., Bodzioch, A. and Fortuny, J. 2019a. Morphology and preliminary biomechanical interpretation of mandibular sutures in Metoposaurus krasiejowensis (Temnospondyli, Stereospondyli) from the Upper Triassic of Poland. *Journal of Iberian Geology*, **45** (2), 301–316.

Gruntmejer, K., Konietzko-Meier, D., Marcé-Nogué, J., Bodzioch, A. and Fortuny, J. 2019b. Cranial suture biomechanics in *Metoposaurus krasiejowensis* (Temnospondyli, Stereospondyli) from the Upper Triassic of Poland. *Journal of Morphology*, **280** (12), 1850–1864.

Gruszka, B. and Zieliński, T. 2008. Evidence for a very low-energy fluvial system: a case study from the dinosaur-bearing Upper Triassic rocks of Southern Poland. *Geological Quarterly*, **52**, 239–252.

Hylander, W.L. 1979. Mandibular function in *Galago crassicaudatus* and *Macaca fascicularis*: An in vivo approach to Stress Analysis of the mandible. *Journal of Morphology*, **159** (2), 253–296.

Janis, C.M., Devlin, K., Warren, D.E. and Witzmann, F. 2012. Dermal bone in early tetrapods: a palaeophysiological hypothesis of adaptation for terrestrial acidosis. *Proceedings of the Royal Society B: Biological Sciences*, **279** (1740), 3035–3040.

Kalita, S., Teschner, E.M., Sander, P.M. and Konietzko-Meier, D. 2022. To be or not to be heavier: The role of dermal bones in the buoyancy of the Late Triassic temnospondyl amphibian *Metoposaurus krasiejowensis*. *Journal of Anatomy*, **241** (6), 1459–1476.

Konietzko-Meier, D., Gruntmejer, K., Marcé-Nogué, J., Bodzioch, A. and Fortuny, J. 2018. Merging cranial histology and 3D-computational biomechanics: a review of the feeding ecology of a Late Triassic temnospondyl amphibian. *PeerJ*, **6**, e4426.

Konietzko-Meier, D. and Klein, N. 2013. Unique growth pattern of Metoposaurus diagnosticus krasiejowensis (Amphibia, Temnospondyli) from the Upper Triassic of Krasiejów, Poland. *Palaeogeography, Palaeoclimatology, Palaeoecology*, **370**, 145–157.

Konietzko-Meier, D. and Sander, P.M. 2013. Long bone histology of *Metoposaurus diagnosticus* (Temnospondyli) from the Late Triassic of Krasiejów (Poland) and its paleobiological implications. *Journal of Vertebrate Paleontology*, **33** (5), 1003–1018.

Konietzko-Meier, D. and Wawro, K. 2007. Mandibular dentition in the Late Triassic temnospondyl amphibian Metoposaurus. *Acta Palaeontologica Polonica*, **52**, 213–215.

Lucas, S. 2015. Age and correlation of Late Triassic tetrapods from southern Poland. *Annales Societatis Geologorum Poloniae*, **85**, 627–635.

Lucas, S.G. 2020. Biochronology of Late Triassic Metoposauridae (Amphibia, Temnospondyli) and the Carnian pluvial episode. *Annales Societatis Geologorum Poloniae*, **90**, 409–418.

Lucas, S.G., Fillmore, D.L. and Simpson, E.L. 2010. Amphibian body impressions from the Mississippian of Pennsylvania, USA. *Ichnos*, **17**, 172–176.

Lucas, S.G., Spielmann, J.A. and Hunt, A.P. 2007. Biochronological significance of Late Triassic tetrapods from Krasiejów, Poland. *New Mexico Museum of Natural History and Science Bulletin*, **41**, 248–258.

Lucas, S.G., Rinehart, L.F., Heckert, A.B., Hunt, A.P. and Spielmann, J.A. 2016. Rotten Hill: A Late Triassic bonebed in the Texas Panhandle, USA. *New Mexico Museum of Natural History and Science Bulletin*, **72**, 1–97.

Lundberg, J.G. and Aguilera, O. 2003. The late Miocene Phractocephalus catfish (Siluriformes: Pimelodidae) from Urumaco, Venezuela: additional specimens and reinterpretation as a distinct species. *Neotropical Ichthyology*, **1** (2), 97–109.

Lydekker, R. 1890. Catalogue of the fossil Reptilia and Amphibia in the British Museum of Natural History. Part IV, 295 pp. British Museum of Natural History; London.

Mader, D. 1997. Palaeoenvironment evolution and bibliography of the Keuper (Upper Triassic) in Germany, Poland and other parts of Europe, 1058 pp. Sven von Loga; Köln.

Märss, T. 2006. Exoskeletal ultrasculpture of early vertebrates. *Journal of Vertebrate Paleontology*, **26** (2), 235–252.

McHenry, C.R., Clausen, P.D., Daniel, W.J.T., Meers, M.B. and Pendharkar, A. 2006. Biomechanics of the rostrum in crocodilians: A comparative analysis using finite-element modeling. *The Anatomical Record Part A: Discoveries in Molecular, Cellular, and Evolutionary Biology*, **288A** (8), 827–849.

McHenry, C.R., Wroe, S., Clausen, P.D., Moreno, K. and Cunningham, E. 2007. Supermodeled sabercat, predatory behavior in *Smilodon fatalis* revealed by high-resolution 3D computer simulation. *Proceedings of the National Academy of Sciences*, **104** (41), 16010–16015.

Metzger, K.A., Daniel, W.J.T. and Ross, C.F. 2005. Comparison of beam theory and finite-element analysis with in vivo bone strain data from the alligator cranium. *The Anatomical Record Part A: Discoveries in Molecular, Cellular, and Evolutionary Biology*, **283A** (2), 331–348.

Meyer, H. von. 1842. Labyrinthodonten-Genera. *Neues Jahrbuch für Mineralogie, Geographie, Geologie, Paläontologie*, **1842**, 301–304.

Meyer, H. von. 1858. Reptilien aus der Steinkohlenformation in Deutschland. *Palaeontographica*, **6**, 59–219.

Milner, A.R. and Schoch, R.R. 2004. The latest metoposaurid amphibians from Europe. *Neues Jahrbuch für Geologie und Paläontologie, Abhandlungen*, **232** (2–3), 231–252.

Olson, E.C. 1961. Jaw Mechanisms: Rhipidistians, Amphibians, Reptiles. *American Zoologist*, **1** (2), 205–215.

Organ, J.M., Ruff, C.B., Teaford, M.F. and Nisbett, R.A. 2006. Do mandibular cross-sectional properties and dental microwear give similar dietary signals? *American Journal of Physical Anthropology*, **130** (4), 501–507.

Pochat-Cottilloux, Y., Martin, J.E., Amiot, R., Cubo, J. and De Buffrénil, V. 2023. A survey of osteoderm histology and ornamentation among Crocodylomorpha: A new proxy to infer lifestyle? *Journal of Morphology*, **284** (1), 1–11.

Racki, G. and Szulc, J. 2015. The bone-bearing Upper Triassic of Upper Silesia, southern Poland: integrated stratigraphy, facies and events – introductory remarks. *Annales Societatis Geologorum Poloniae*, **85**, 553–555.

Rayfield, E.J. 2007. Finite Element Analysis and Understanding the Biomechanics and Evolution of Living and Fossil Organisms. *Annual Review of Earth and Planetary Sciences*, **35** (1), 541–576.

Rinehart, L.F. and Lucas, S.G. 2013a. The functional morphology of dermal bone ornamentation in temnospondyl amphibians. In: Tanner, L.H., Spielmann, J.A. and Lucas, S.G. (Ed.), The Triassic System, Vol. 61, 524–532. New Mexico Museum of Natural History and Science Bulletin; Albuquerque.

Rinehart, L.F. and Lucas, S.G. 2013b. Tooth form and function in temnospondyl amphibians: Relationship of shape to applied stress. In: Tanner, L.H., Spielmann, J.A. and Lucas, S.G. (Eds), The Triassic System. *New Mexico Museum of Natural History and Science, Bulletin*, **61**, 533–542.

Rinehart, L.F. and Lucas, S.G. 2016. *Eocyclotosaurus appetolatus*, a Middle Triassic Amphibian: Osteology, life history, and paleobiology. *New Mexico Museum of Natural History and Science Bulletin*, **70**, 1–118.

Rinehart, L.F. and Lucas, S.G. 2023. Lateral skull angle: a new sexual dimorphism signal in temnospondyl amphibians. *New Mexico Museum of Natural History and Science Bulletin*, **84**, 559–584.

Rinehart, L.F., Lucas, S.G., Hunt, A.P. and Heckert, A.B. 2023. Skull and jaw shape as indicators of trophic guild association in temnospondyl amphibians and other aquatic predators. *New Mexico Museum of Natural History and Science Bulletin*, **94**, 585–610.

Romer, A.S. 1947. Review of the Labyrinthodontia. *Bulletin of the Museum of Comparative Zoolology, Harvard University*, **99**, 1–368.

Rowe, A.J. and Snively, E. 2022. Biomechanics of juvenile tyrannosaurid mandibles and their implications for bite force: Evolutionary biology. *The Anatomical Record*, **305** (2), 373–392.

Ruta, M. and Bolt, J.R. 2008. The brachyopoid Hadrokkosaurus bradyi from the early Middle Triassic of Arizona, and a phylogenetic analysis of lower jaw characters in temnospondyl amphibians. *Acta Palaeontologica Polonica*, **53**, 579–592.

Scheyer, T., Martinsander, P., Joyce, W., Bohme, W. and Witzel, U. 2007. A plywood structure in the shell of fossil and living soft-shelled turtles (Trionychidae) and its evolutionary implications. *Organisms Diversity & Evolution*, **7** (2), 136–144.

Schoch, R.R. 2001. Can metamorphosis be recognised in Palaeozoic amphibians ? *Neues Jahrbuch für Geologie und Paläontologie, Abhandlungen*, **220** (3), 335–367.

Schoch, R.R. 2009. Life-cycle evolution as response to diverse lake habitats in Paleozoic amphibians. *Evolution*, **63** (10), 2738–2749.

Schoch, R.R. 2009b. Evolution of life cycles in early amphibians. *Annual Review of Earth and Planetary Sciences*, **37**, 135–162.

Schoch, R.R. 2010. Heterochrony: the interplay between development and ecology exemplified by a Paleozoic amphibian clade. *Paleobiology*, **36**, 318–334.

Schultze, H.P. and Arsenault, M. 1985. The panderichthyid fish *Elpistostege*: A close relative of tetrapods? *Palaeontology*, **28**, 293–309.

Seibert, E.A., Lillywhite, H.B. and Wassersug, R.J. 1974. Cranial co-ossification in frogs: relationship to rate of evaporite water loss. *Physiological Zoology*, **47**, 261–265.

Seidel, M.R. 1979. The osteoderms of the American alligator and their functional significance. *Herpetologica*, **35**, 375–380.

Settle, R.A., Briggler, J.T. and Mathis, A. 2018. A quantitative field study of paternal care in Ozark hellbenders, North America's giant salamanders. *Journal of Ethology*, **36**, 235–242.

Shine, R. 1979. Sexual selection and sexual dimorphism in the amphibian. *Copeia*, **1979** (2), 297–306.

Slater, G.J., Dumont, E.R. and Van Valkenburgh, B. 2009. Implications of predatory specialization for cranial form and function in canids. *Journal of Zoology*, **278** (3), 181–188.

Slater, G.J., Figueirido, B., Louis, L., Yang, P. and Van Valkenburgh, B. 2010. Biomechanical Consequences of Rapid Evolution in the Polar Bear Lineage. *PLoS ONE*, **5** (11), e13870.

Snively, E., Henderson, D.M. and Phillips, D.S. 2006. Fused and vaulted nasals of tyrannosaurid dinosaurs: Implications for cranial strength and feeding mechanics. *Acta Palaeontologica Polonica*, **51**, 435–454.

Środoń, J., Szulc, J., Anczkiewicz, A., Jewuła, K., Banaś, M. and Marynowski, L. 2014. Weathering, sedimentary and diagenetic controls of mineral and geochemical characteristics of the vertebrate-bearing Silesian Keuper. *Clay Minerals*, **49** (4), 569–594.

Sulej, T. 2002. Species discrimination of the Late Triassic temnospondyl amphibian Metoposaurus diagnosticus. *Acta Palaeontologica Polonica*, **47**, 535–546.

Sulej, T. 2007. Osteology, variability, and evolution of Metoposaurus, a temnospondyl from the Late Triassic of Poland. *Paleontologia Polonica*, **64**, 29–139.

Sulej, T. and Majer, D. 2005. The temnospondyl amphibian *Cyclotosaurus* from the Upper Triassic of Poland. *Palaeontology*, **48** (1), 157–170.

Szulc, J., Racki, G. and Jewuła, K. 2015a. Key aspects of the stratigraphy of the Upper Silesian middle Keuper, southern Poland. *Annales Societatis Geologorum Poloniae*, **85**, 557–586.

Szulc, J., Racki, G., Jewuła, K. and Środoń, J. 2015b. How

many Upper Triassic bone-bearing levels are there in Upper Silesia (southern Poland)? A critical overview of stratigraphy and facies. *Annales Societatis Geologorum Poloniae*, **85**, 587–626.

Teschner, E.M., Sander, P.M. and Konietzko-Meier, D. 2018. Variability of growth pattern observed in *Metoposaurus krasiejowensis* humeri and its biological meaning. *Journal of Iberian Geology*, **44**, 99–111.

Therrien, F. 2005a. Feeding behaviour and bite force of sabretoothed predators. *Zoological Journal of the Linnean Society*, **145** (3), 393–426.

Therrien, F. 2005b. Mandibular force profiles of extant carnivorans and implications for the feeding behaviour of extinct predators. *Journal of Zoology*, **267** (3), 249–270.

Therrien, F., Henderson, D.M. and Ruff, C.B. 2005. Bite me: Biomechanical models of theropod mandibles and implications for feeding behavior. In: Carpenter, K. (Ed.), The Carnivorous Dinosaurs, 179–237. Indiana University Press; Bloomington.

Therrien, F., Quinney, A., Tanaka, K. and Zelenitsky, D.K. 2016. Accuracy of mandibular force profiles for bite force estimation and feeding behavior reconstruction in extant and extinct carnivorans. *Journal of Experimental Biology*, **219** (23), 3738–3749.

Timoshenko, S.P. and Gere, J.M. 1972. Mechanics of Materials, 556 pp. Van Nostrand Reinhold Company; New York.

Tseng, Z.J. 2013. Testing adaptive hypotheses of convergence with functional landscapes: a case study of bone-cracking hypercarnivores. *PLoS ONE*, **8** (5), e65305.

Tseng, Z.J. and Binder, W.J. 2010. Mandibular biomechanics of *Crocuta crocuta*, *Canis lupus*, and the late Miocene *Dinocrocuta gigantea* (Carnivora, Mammalia): *Dinocrocuta* mandibular biomechanics. *Zoological Journal of the Linnean Society*, **158** (3), 683–696.

Tseng, Z.J. and Wang, X. 2010. Cranial functional morphology of fossil dogs and adaptation for durophagy in *Borophagus* and *Epicyon* (Carnivora, Mammalia). *Journal of Morphology*, **271** (11), 1386–1398.

Tseng, Z.J., Antón, M. and Salesa, M.J. 2011. The evolution of the bone-cracking model in carnivorans: cranial functional morphology of the Plio-Pleistocene cursorial hyaenid *Chasmaporthetes lunensis* (Mammalia: Carnivora). *Paleobiology*, **37** (1), 140–156.

Vági, B., Marsh, D., Katona, G., Végvári, Z., Freckleton, R.P., Liker, A. and Székely, T. 2022. The evolution of parental care in salamanders. *Scientific Reports*, **12** (1), 16655.

Vorobyeva, E.I. and Schultze, H.P. 1991. Description and systematics of panderichthyid fishes with comments on their relationship to tetrapods. In: Schultze, H-P. and Trueb, L. (Ed.), Origins of Higher Groups of Tetrapods, 68–109. Comstock Publishing Associates; Ithaca.

Walmsley, C.W., Smits, P.D., Quayle, M.R., McCurry, M.R., Richards, H.S., Oldfield, C.C.,

Wroe, S., Clausen, P.D. and McHenry, C.R. 2013. Why the long face? The mechanics of mandibular symphysis proportions in crocodiles. *PLoS ONE*, **8** (1), e53873.

Watson, D.M.S. 1919. The structure, evolution and origin of the Amphibia. The 'Orders' Rachitomi and Stereospondyli. *Philosophical Transaction of the Royal Society of London, Series B*, **209**, 1–73.

Weryński, Ł. and Kędzierski, M. 2022. Microstructural characteristics and seasonal growth patterns observed in Metoposaurus krasiejowensis teeth. *Geological Quarterly*, **66**, 26.

Westoll, T.S. 1938. Ancestry of the Tetrapods. *Nature*, **141**, 127–128.

Whiteaves, J.F. 1881. On some remarkable fossil fishes from the Devonian rocks of Scaumenac Bay, in the Province of Quebec. *Annals and Magazine of Natural History*, **8** (44), 159–162.

Witzmann, F. and Gassner, T. 2008. Metoposaurid and mastodonsaurid stereospondyls from the Triassic–Jurassic boundary of Portugal. *Alcheringa: An Australasian Journal of Palaeontology*, **32** (1), 37–51.

Witzmann, F. and Soler-Gijón, R. 2010. The bone histology of osteoderms in temnospondyl amphibians and in the chroniosuchian *Bystrowiella*. *Acta Zoologica*, **91** (1), 96–114.

Witzmann, F., Scholz, H., Müller, J. and Kardjilov, N. 2010. Sculpture and vascularization of dermal bones, and the implications for the physiology of basal tetrapods. *Zoological Journal of the Linnean Society*, **160** (2), 302–340.

Wroe, S., Clausen, P., McHenry, C., Moreno, K. and Cunningham, E. 2007. Computer simulation of feeding behaviour in the thylacine and dingo as a novel test for convergence and niche overlap. *Proceedings of the Royal Society B: Biological Sciences*, **274** (1627), 2819–2828.

Yates, A.M. and Warren, A.A. 2000. The phylogeny of the "higher" temnospondyls (Vertebrata: Choanata) and its implications for the monophyly and origins of the Stereospondyli. *Zoological Journal of the Linnean Society*, **128**, 77–121.

Young, G.C. 2009. An Ordovician vertebrate from western New South Wales, with comments on Cambro-Ordovician vertebrate distribution patterns. *Alcheringa: An Australasian Journal of Palaeontology*, **33** (1), 79–89.

Zittel, K.A. von. 1911. Grundzüge der Paläontologie (Paläozoologie). II. Abteilung. Vertebrata, 576 pp. Verlag von R. Oldenbourg; München and Berlin.

Zylberberg, L., Meunier, F.J. and Laurin, M. 2010. A Microanatomical and Histological Study of the Postcranial Dermal Skeleton in the Devonian Sarcopterygian *Eusthenopteron foordi*. *Acta Palaeontologica Polonica*, **55**, 459–470.

Manuscript submitted: 22nd February 2024
Revised version accepted: 26th June 2024

Appendix 1

Mandible measurements in mm and categorical variables for *Metoposaurus krasiejowensis* Sulej, 2002 (22 specimens) and *Cyclotosaurus intermedius* Sulej and Majer, 2005 (UO2BP5V).

invnum	side	sr	pst	tusk	st	er	ao	antp	l1	l2	ld	h1	h2	h3	h4	h5
UOBS01264	right	N	N	N	N	N	low	0	287	287	188	48.3	63.8	67.6	0	66.7
UOBS02059	right	Y	Y	Y	post	Y	low	0	300	317	240	42.6	42.6	52.7	11.2	52.4
UOBS02060	right	Y	Y	Y	post	N	high	3.7	340	380	285	49.8	58.6	63	12.9	59.6
UOBS02061	right	Y	Y	Y	post	N	low	4.8	350	368	270	54.2	54.6	58.6	12.5	60.5
UOBS02062	right	Y	Y	Y	post	N	low	6.1	365	405	300	48.7	49.8	61	15.4	63.4
UOBS02063	left	N	N	N	N	N	low	0	290	305	210	48.2	48.8	57.5	0	55.4
UOBS02064	left	N	N	N	N	N	low	0	280	290	200	51.9	53.6	59.4	0	59.7
UOBS02065	left	N	N	N	N	N	low	0	300	300	210	47.1	52.9	59.9	0	59.6
UOBS02066	left	N	N	N	N	N	low	0	270	270	165	46.4	47.2	58.1	0	56.3
UOBS03023	left	Y	Y	Y	ant	N	low	4	500	530	390	74.3	84.7	87.4	25.5	86.8
UOPB3487	left	N	N	N	N	N	low	0	0	0	0	37.9	45.3	58.2	0	0
UOPB3488	right	Y	Y	Y	post	N	high	2.6	325	355	0	46.2	53.4	60	11.9	0
UOPB3489	left	N	N	N	N	N	low	0	0	0	0	43.8	43.8	52.2	0	0
UOPB3490	left	Y	Y	N	N	N	high	3.5	400	430	0	58.3	58.3	75.9	14.7	0
UOPB3493	left	Y	N	N	N	N	low	0	335	365	275	50	60.5	67.7	9.8	65.2
UOPB3494	left	Y	Y	Y	post	N	low	0	300	328	245	41.1	48.9	53.6	10.6	53.1
UOPB3497	left	Y	Y	N	N	N	high	0	330	355	0	52.2	58	61.8	13.3	0
UOPB3498	left	Y	N	N	N	N	low	0	290	300	0	45.8	53.2	56.6	0	0
UOPB3502	left	Y	N	N	N	N	low	0	280	300	210	37.2	0	46.3	9.7	45.3
UOPB3503	left	Y	Y	Y	ant	Y	high	4.3	405	440	330	53.2	62.9	81.2	15.9	71.7
UOPB3504	left	Y	Y	Y	ant	N	high	5.4	390	435	315	57	61.6	65.3	17.2	64.2
UOPB3505	left	Y	Y	Y	ant	N	N	0	0	0	0	0	0	0	14	0
UO2BP5V	left	Y	Y	N	N	N	low	0	670	720	565	115	148	118	37.3	120

invnum	h6	a	m	hm	d1	l3	h7	d2	l4	h8	d3	l5	h9	w1	w2	w3
UOBS01264	0	73.8	59.2	15.9	14.6	5.4	2.7	17.4	4	2	0	0	0	36.4	0	0
UOBS02059	37.8	66.1	43.6	12.9	21.6	5.3	2.2	8	9.4	2.5	0	0	0	29.8	13.4	18.7
UOBS02060	39.2	79.3	56.3	15.5	13.5	5.3	2.5	23.7	6.5	2.9	0	0	0	38.5	19.7	24.9
UOBS02061	38	71.5	47.1	14	26	3.4	1.8	21.6	6.5	5.7	0	0	0	37.5	13.9	23.4
UOBS02062	45.7	86.8	0	15	13.5	1.7	1.8	22.7	2.9	1.4	26	4.7	2.3	42.6	23.1	31.8
UOBS02063	0	76	47.2	13.6	17.6	5.6	0	0	0	0	0	0	0	37.1	15.6	0
UOBS02064	0	68	47.7	14.7	0	0	0	0	0	0	0	0	0	30.1	12.5	0
UOBS02065	0	69.2	52.5	17	19.8	6.2	2.3	17.4	6.3	3.6	0	0	0	30	13.8	0
UOBS02066	0	69	68.5	21	0	0	0	0	0	0	0	0	0	32.8	13	0
UOBS03023	54.3	102	66.3	16.5	26.1	1.4	1.3	58.5	5	3	0	0	0	62.1	21	36.1
UOPB3487	0	56.9	0	0	0	0	0	0	0	0	0	0	0	40.9	13.7	0
UOPB3488	0	67.4	40.6	15	25.2	2.1	1.6	21.8	3.1	1.3	0	0	0	35.8	13.2	22.9
UOPB3489	0	68.3	0	0	0	0	0	0	0	0	0	0	0	25.2	0	0
UOPB3490	0	87.5	64.8	15	22.5	7.2	2.3	8.9	2.6	1.7	8	10.4	3.4	25.5	14.5	26.8
UOPB3493	39.8	73	55	0	15	3.2	1.5	35.4	3.2	1.8	0	0	0	39.2	17.6	27.6
UOPB3494	29.1	66.9	45.5	12.6	0	0	0	0	0	0	0	0	0	37.4	12.5	22.2
UOPB3497	0	67.3	62.8	14.8	13.9	1.5	1	24.5	5.5	2.1	0	0	0	38.3	14.9	24.3
UOPB3498	0	67.9	46.8	14.4	22.1	2.8	1.4	20.1	5.2	2.4	0	0	0	29.3	12.3	0
UOPB3502	26.4	0	0	0	0	0	0	0	0	0	0	0	0	0	0	0
UOPB3503	39.2	88.1	61.7	17	22.7	3.4	2.2	35	5.3	3.7	0	0	0	37.7	18	29.1
UOPB3504	40	85.5	61.4	15.3	26.2	3.9	1	27.8	8.5	2.7	0	0	0	43	18.6	28.6
UOPB3505	0	0	0	0	0	0	0	0	0	0	0	0	0	0	15.4	23.4
UO2BP5V	70.2	163	87.1	33.5	66	3.6	3.7	44.9	5.6	4.6	0	0	0	92	30.2	45.9

invnum	w4	w5	wa	w6	h10	l6	l7	l8	l9	1	2	3	4
UOBS01264	19.3	0	7.9	0	0	0	0	76.8	90.9	N	N	N	N
UOBS02059	23.6	13.8	12	18.4	9.6	295	180	60	75.8	irregular	dense	small	constant
UOBS02060	27.7	17.6	9	21.7	13	337	200	60	90	irregular	dense	small	variable
UOBS02061	35.2	15.3	16	22.9	13.8	328	200	65	80	regular	dense	small	constant
UOBS02062	37.5	19.6	18	29.3	15.8	375	238	88	103	regular	vsparse	vlarge	constant
UOBS02063	31	0	18.2	0	0	0	0	0	87	N	N	N	N
UOBS02064	25.7	0	12.1	0	0	0	0	55	67	regular	dense	large	constant
UOBS02065	17.8	0	5.2	0	0	0	0	0	85	N	N	N	N
UOBS02066	22.8	0	10.9	0	0	0	0	75	80	regular	sparse	large	variable
UOBS03023	42.7	24.3	33.7	36.5	27.8	485	295.9	100	100	irregular	sparse	vlarge	constant
UOPB3487	0	0	20.4	0	0	0	0	0	0	N	N	N	N
UOPB3488	0	0	18.2	22.8	11.1	317	0	0	83	N	N	N	N
UOPB3489	0	0	18.2	0	0	0	0	0	0	N	N	N	N
UOPB3490	0	0	13.7	0	0	0	0	100	0	N	N	N	N
UOPB3493	26.5	16.3	15	26.4	13.7	330	200	60	85	regular	sparse	vlarge	constant
UOPB3494	31.1	14	19	21.9	11.7	300	180	60	70	N	N	N	N
UOPB3497	0	0	19.9	21.5	13.3	315	0	0	0	N	N	N	N
UOPB3498	0	0	9.7	0	0	0	0	0	0	N	N	N	N
UOPB3502	0	0	0	0	0	0	0	0	0	N	N	N	N
UOPB3503	31.8	15.6	17.8	29.5	17.6	393	235	75	130	irregular	sparse	vlarge	variable
UOPB3504	35.1	18.8	24.3	28.9	16.3	395	240	85	100	irregular	dense	large	constant
UOPB3505	0	0	0	22.2	15.5	0	0	0	0	N	N	N	N
UO2BP5V	54.6	38.4	23.5	45.5	37	630	355	80	65	irregular	vsparse	vlarge	variable

invnum	5	6	7	8	9	10	11	12	13
UOBS01264	N	N	N	N	N	N	N	N	N
UOBS02059	deepshallow	same	constant	fine	narrow	nobroad	rounded	radial	polygonalrounded
UOBS02060	deep	same	constant	fine	narrow	nobroad	rounded	radial	polygonalrounded
UOBS02061	deepshallow	same	constant	coarse	variable	nobroad	rounded	sculptural	polygonalrounded
UOBS02062	shallow	same	variable	coarse	narrow	nobroad	rounded	sculptural	polygonal
UOBS02063	N	N	N	N	N	N	N	N	N
UOBS02064	deep	same	constant	coarse	variable	nobroad	rounded	radial	polygonalrounded
UOBS02065	N	N	N	N	N	N	N	N	N
UOBS02066	deep	same	constant	fine	narrow	nobroad	rounded	sculptural	polygonalrounded
UOBS03023	deepshallow	same	constant	fine	narrow	nobroad	rounded	radial	polygonal
UOPB3487	N	N	N	N	N	N	N	N	N
UOPB3488	N	N	N	N	N	N	N	N	N
UOPB3489	N	N	N	N	N	N	N	N	N
UOPB3490	N	N	N	N	N	N	N	N	N
UOPB3493	deepshallow	same	variable	coarse	narrow	nobroad	rounded	sculptural	polygonal
UOPB3494	N	N	N	N	N	N	N	N	N
UOPB3497	N	N	N	N	N	N	N	N	N
UOPB3498	N	N	N	N	N	N	N	N	N
UOPB3502	N	N	N	N	N	N	N	N	N
UOPB3503	deepshallow	same	constant	coarse	narrow	nobroad	rounded	sculptural	polygonal
UOPB3504	deepshallow	same	constant	coarse	narrow	nobroad	rounded	sculptural	polygonal
UOPB3505	N	N	N	N	N	N	N	N	N
UO2BP5V	deep	samelow	variable	coarse	narrow	nobroad	rounded	radial	polygonal

invnum	14	15	16	17	18
UOBS01264	N	N	N	N	N
UOBS02059	others	multipolygons	notubercles	present	absent
UOBS02060	pentagons	none	notubercles	present	present
UOBS02061	others	multipolygons	notubercles	absent	absent
UOBS02062	others	none	notubercles	absent	absent
UOBS02063	N	N	N	N	N
UOBS02064	others	none	notubercles	present	absent
UOBS02065	N	N	N	N	N
UOBS02066	others	multipolygons	notubercles	absent	absent
UOBS03023	others	multipolygons	notubercles	absent	absent
UOPB3487	N	N	N	N	N
UOPB3488	N	N	N	N	N
UOPB3489	N	N	N	N	N
UOPB3490	N	N	N	N	N
UOPB3493	others	multipolygons	notubercles	present	absent
UOPB3494	N	N	N	N	N
UOPB3497	N	N	N	N	N
UOPB3498	N	N	N	N	N
UOPB3502	N	N	N	N	N
UOPB3503	others	multipolygons	notubercles	present	absent
UOPB3504	others	multipolygons	notubercles	absent	absent
UOPB3505	N	N	N	N	N
UO2BP5V	others	multipolygons	notubercles	present	present

Appendix 2

Complete explanation of mandibular force profile method from Therrien *et al.* (2005).

The simplified model of the ramus of the mandible is a solid beam with elliptical section. The axes of the ellipse are the labiolingual axis, *x*, and the dorsoventral axis, *y*, of the mandible. The second moment of area, *I*, is a measure of the distribution of bones around an axis and can be expressed as:

$I = \int y^2 dA$

where *dA* is an elemental strip of area and *y* is the distance of the elemental strip from the centroid, or neutral axis, of the mandible. The formula can be simplified to:

$Ix = \pi ba^3/4$, for labiolingual axis (in cm^4)

$Iy = \pi ab^3/4$, for dorsoventral axis (in cm^4)

where *a* is the dorsoventral radius and *b* the labiolingual radius (Biewener 1992). The section modulus, *Z*, is a measure of the strength in bending and can be expressed as:

$Z = I/y$

where *I* is the second moment area and *y* is the distance of the centroid from the outer edge of the bone in the plane of bending or radius of the corpus (Biknevicius and Ruff 1992). Then, for the two axes, *Z* can be expressed as:

$Zx = Ix/a$, bending strength in the dorsoventral plane, or about labiolingual axis (in cm^3)

$Zy = Ix/b$, bending strength in the labiolingual plane, or about dorsoventral axis (in cm^3).

The maximum bending stress, σB, can be expressed as:

$\sigma_B = My/I$

where *M* is the bending moment, *y* is the radius orthogonal to the axis investigated and *I* the second moment of the area about the axis investigated. The bending stress depends on the material, but here it is constant, then:

$M = I/y = Z$.

The bending moment can be expressed as:

$M = FL$

where *F* is the applied force and *L* is the moment arm length (Timoshenko and Gere 1972). But $M = Z$, so:

$Z = FL$

$F = Z/L$ (in cm^2).